



Ozone Monitoring Instrument (OMI) Data User's Guide

OMI-DUG-1.0
February 5, 2008



This page is blank to preserve correct left-right pagination.



Contents

CHAPTER 1: BEFORE YOU BEGIN	1
1.1 PURPOSE OF THE DOCUMENT	1
1.2 ACRONYMS, ABBREVIATIONS, AND DEFINITIONS	1
1.3 OVERVIEW OF THE DOCUMENT	3
CHAPTER 2: THE OZONE MONITORING INSTRUMENT	5
2.1 INTRODUCTION TO THE OMI	5
2.2 THE AURA MISSION	6
2.3 OMI MISSION OBJECTIVES	6
2.4 OMI DESCRIPTION	7
2.4.1 <i>Main Elements</i>	7
2.4.2 <i>Measurement Principle</i>	8
2.4.3 <i>Observation Modes</i>	10
CHAPTER 3: OMI DATA PRODUCTS	13
3.1 OMI DATA PROCESSING AND PRODUCT SUMMARY	13
3.2 LEVEL 1B PRODUCTS: OMI RADIOMETRICALLY CALIBRATED AND GEO-LOCATED RADIANCE PRODUCTS	13
3.3 LEVEL 2 PRODUCTS: OMI ORBITAL ATMOSPHERIC PRODUCTS	15
3.3.1 <i>Ozone Products</i>	16
3.3.2 <i>Clouds, Aerosols and Surface UV Irradiance Products</i>	17
3.3.3 <i>Trace Gases Products</i>	20
3.4 LEVEL 2G PRODUCTS	21
3.5 LEVEL 3 PRODUCTS: OMI GLOBAL GRIDDED ATMOSPHERIC PRODUCTS	22
CHAPTER 4: QUALITY ASSESSMENT OF OMI LEVEL 2 PRODUCTS	23
4.1 OMI PIXEL SIZE	23
4.2 OMI/AURA AEROSOL EXTINCTION OPTICAL DEPTH AND AEROSOL TYPES (OMAERO)	28
4.2.1 <i>Quality Assessment</i>	28
4.2.2 <i>Additional Information</i>	30
4.3 OMI/AURA AEROSOL EXTINCTION AND ABSORPTION OPTICAL DEPTH (OMAERUV)	30
4.3.1 <i>Quality Assessment</i>	30
4.3.2 <i>Additional Information</i>	32
4.4 OMI/AURA BROMINE MONOXIDE TOTAL COLUMN (OMBRO)	33
4.4.1 <i>Quality Assessment</i>	33
4.4.2 <i>Additional Information</i>	34
4.5 OMI/AURA CLOUD PRESSURE AND FRACTION (O ₂ -O ₂ ABSORPTION) (OMCLDO2)	35
4.5.1 <i>Quality Assessment</i>	35
4.5.2 <i>Additional Information</i>	35
4.6 OMI/AURA CLOUD PRESSURE AND FRACTION (RAMAN SCATTERING) (OMCLDRR)	36
4.6.1 <i>Quality Assessment</i>	36
4.6.2 <i>Algorithm Quality Assessment</i>	37
4.6.3 <i>Additional Information</i>	38
4.7 OMI/AURA DOAS TOTAL COLUMN OZONE (OMDOAO3)	39
4.7.1 <i>Quality Assessment</i>	39
4.7.2 <i>Additional Information</i>	39
4.8 OMI/AURA FORMALDEHYDE (HCHO) TOTAL COLUMN (OMHCHO)	40
4.8.1 <i>Quality Assessment</i>	40
4.8.2 <i>Additional Information</i>	40
4.9 OMI/AURA NITROGEN DIOXIDE (NO ₂) TOTAL AND TROPOSPHERIC COLUMN (OMNO2)	41
4.9.1 <i>Quality Assessment</i>	41



4.9.2 Additional Information.....	41
4.10 OMI/AURA CHLORINE DIOXIDE SLANT COLUMN (OMOCLO).....	42
4.10.1 Quality Assessment.....	42
4.10.2 Additional Information.....	42
4.11 OMI/AURA SULFUR DIOXIDE TOTAL COLUMN (OMSO2).....	42
4.11.1 Quality Assessment.....	42
4.11.2 Additional Information.....	45
4.12 OMI/AURA OZONE (O ₃) TOTAL COLUMN (OMTO3).....	45
4.12.1 Quality Assessment.....	45
4.12.2 Additional Information.....	46
4.13 OMI/AURA SURFACE UV IRRADIANCES (OMUVB).....	46
4.13.1 Quality Assessment.....	46
4.13.2 Additional Information.....	46
CHAPTER 5: OMI DATA ACCESS AND USE.....	47
5.1 DATA FORMAT.....	47
5.2 ACCESSING OMI DATA.....	47
5.3 USING OMI DATA.....	48
5.4 EXAMPLE OF USAGE.....	49
CHAPTER 6: REFERENCES.....	51
6.1 OMI ALGORITHMIC THEORETICAL BASELINE DOCUMENTS (ATBDs).....	51
6.2 ADDITIONAL REFERENCES.....	51



Chapter 1: Before You Begin

1.1 Purpose of the Document

Researchers and scientists in atmospheric sciences use this document to understand Ozone Monitoring Instrument (OMI) data and the OMI data products available. Most readers have with some background in atmospheric physics or chemistry, but not necessarily a strong background in remote sensing.

This guide provides the following:

- 1) Descriptions of the origin, advantages and limitations of the OMI.
- 2) Descriptions of OMI data products and their use.

The sources of information compiled for this document are listed in “Chapter 6: References,” beginning on Page 51.

1.2 Acronyms, Abbreviations, and Definitions

AAOD	Aerosol Absorption Optical Depth
AOD	Aerosol Extinction Optical Depth
AERONET	Aerosol Robotic Network
AQUA	The First Member Satellite in A-Train Series
ATSR	Along Track Scanning Radiometer
BRD	Band Residual Difference
BUV	Backscatter Ultraviolet
CCD	Charge-Coupled Device
DAAC	Distributed Active Archive Center
DEM	Detector Module
DU	Dobson Unit
ELU	Electronics Unit
EOS	Earth Observing System
EP	Earth Probe (satellite)
FOV	Field of View
FWHM	Full Width at Half Maximum
GDPS	Ground Data Processing System
GES DISC	Goddard Earth Sciences Data and Information Services Center
GEOS	Goddard Earth Observing System



GEOS-CHEM	A global three-dimensional model of atmospheric composition driven by assimilated meteorological observations from GEOS
GOME	Global Ozone Monitoring Experiment
HDF	Hierarchical Data Format, current level HDF5
HDF-EOS	The prescribed format for standard data products derived from EOS missions
IAM	Interface Adaptor Module
Ifov	Instantaneous Field of View
L0	Level 0 data are reconstructed, unprocessed instrument and payload data at full resolution, after the removal of all communications artifacts (for example, synchronization frames, communications headers, duplicate data). In most cases, the EOS Data and Operations System (EDOS) provides these data to the DAACs as production datasets for processing by the Science Data Processing Segment (SDPS) or by a SIPS to produce higher level products.
For more specific information about L0 through L3 data, refer to “Chapter 3: OMI Data Products” beginning on Page 13.	
L1A	Level 1A datasets consist of Level 0 data that have been time-referenced and annotated with ancillary information, including radiometric and geometric calibration coefficients and georeferencing parameters (for example, platform ephemeris) computed and appended but not applied to the Level 0 data.
L1B	Level 1B datasets consist of Level 1A data that have been processed to sensor units.
L2	Level 2 datasets contain derived geophysical variables at the same resolution and location as the Level 1 source data.
L2G	Level 2G datasets contain one day's worth of the Level 2 data (typically 14 orbits) ordered by ground position rather than by time.
L3	Level 3 data consists of L2 datasets with the variables mapped on uniform space-time grid scales, usually with some completeness and consistency.
LER	Lambertian-Equivalent Reflectivity
LF	Linear Fit
LIDAR	Light Detection and Ranging
LUT	Look-Up Table
MLER	Mixed Lambertian-Equivalent Reflectivity



MODIS	MODerate resolution Imaging Spectrometer
NIMBUS	A series of satellites for meteorological research
OA	Optical Assembly
OPB	Optical Bench
OMI	Ozone Monitoring Instrument
PBL	Planetary Boundary Layer
QF	Quality Flag
RMS	Root-Mean-Square (power measurement)
SBUV	Solar Backscatter Ultraviolet (instrument)
SC	Slant Column
SCO	Slant Column Ozone
SF	Spectral Fit
SIPS	Science Investigator-led data Processing System
SNR	Signal-to-Noise Ratio
SSA	Single Scattering Albedo
SZA	Solar Zenith Angle
TOMS	Total Ozone Mapping Spectrometer
UV	Ultra Violet
UVAI	UV Aerosol Index
VIS	Visible
Symbols:	Definitions:
σ	Standard Deviation
τ	Cloud Optical Depth

1.3 Overview of the Document

The chapters in this guide are described below:

Chapter 1 is the introduction to the guide.

Chapter 2 gives general information about the OMI.

Chapter 3 describes OMI data products in general.

Chapter 4 describes quality assessments of OMI Level 2 data products.

Chapter 5 describes OMI data format, data access and data usage.

Chapter 6 provides a reference list of source documents.



This page is blank to preserve correct left-right pagination.



Chapter 2: The Ozone Monitoring Instrument

2.1 Introduction to the OMI

OMI is a nadir-viewing near-UV/Visible CCD spectrometer aboard NASA's Earth Observing System's (EOS) Aura satellite. Aura flies in formation about 15 minutes behind Aqua, both of which orbit the earth in a polar Sun-synchronous pattern. Aura was launched on July 15, 2004, and OMI has collected data since August 9, 2004.

OMI measurements cover a spectral region of 264–504 nm (nanometers) with a spectral resolution between 0.42 nm and 0.63 nm and a nominal ground footprint of $13 \times 24 \text{ km}^2$ at nadir. Essentially complete global coverage is achieved in one day. The significantly improved spatial resolution of OMI measurements as well as the vastly increased number of wavelengths observed, as compared to TOMS, GOME and SCIAMACHY, sets a new standard for trace gas and air quality monitoring from space. The OMI observations provide the following capabilities and features:

- A mapping of ozone columns at $13 \text{ km} \times 24 \text{ km}$ and profiles at $13 \text{ km} \times 48 \text{ km}$ (a continuation of TOMS and GOME ozone column data records and the ozone profile records of SBUV and GOME)
- A measurement of key air quality components: NO_2 , SO_2 , BrO, HCHO, and aerosol (a continuation of GOME measurements)
- The ability to distinguish between aerosol types, such as smoke, dust and sulfates
- The ability to measure aerosol absorption capacity in terms of aerosol absorption optical depth or single scattering albedo
- A measurement of cloud pressure and coverage
- A mapping of the global distribution and trends in UV-B radiation
- A combination of processing algorithms including TOMS Version 8, DOAS (Differential Optical Absorption Spectroscopy), Hyperspectral BUV retrievals and forward modeling to extract the various OMI data products
- Near real-time measurements of ozone and other trace gases

The OMI is a contribution of NIVR (Netherlands Institute for Air and Space Development) of Delft, in collaboration with FMI (Finnish Meteorological Institute), Helsinki, Finland, to the EOS Aura mission. The Dutch industrial efforts focused on the optical bench design and assembly, thermal design and project management. The detector modules and the readout and control electronics were provided by Finnish industrial partners.



2.2 The Aura Mission

Aura is the atmospheric chemistry mission of NASA's three-platform Earth Observing System (EOS) with the overall objective of studying the chemistry and dynamics of Earth's atmosphere from the ground through the mesosphere. The goal is to monitor the complex interactions of atmospheric constituents that are contributing to global change and to the creation and depletion of ozone. These atmospheric constituents are both from natural sources, such as biological activity and volcanoes, and from man-made sources, such as biomass burning.

The Aura satellite orbits at an altitude of 705 km in a sun-synchronous polar orbit with an exact 16-day repeat cycle and with a local equator crossing time of 13.45 (1:45 P.M.) on the ascending node. The orbital inclination is 98.1 degrees, providing latitudinal coverage from 82° N to 82° S.

Apart from OMI, the Aura satellite also carries onboard three other instruments: the High Resolution Dynamics Limb Sounder (HIRDLS), the Microwave Limb Sounder (MLS) and the Tropospheric Emission Spectrometer (TES). For more information about Aura and its instruments, refer to the Aura website (<http://aura.gsfc.nasa.gov/>). OMI calibration and validation information can be found in Dobber et al. (2006) and Froidevaux and Douglass (2001).

Algorithmic theoretical basis documents (ATBD) for OMI and other Aura instruments are available at http://eospsos.gsfc.nasa.gov/eos_homepage/for_scientists/atbd/

2.3 OMI Mission Objectives

OMI's scientific mission (objectives discussed in detail by Levelt, et al., 2006) is directly related to the Aura mission objectives. The OMI mission seeks answers to the following questions:

- Is the ozone layer recovering as expected?
- What are the sources of aerosols and trace gases that affect global air quality and how are they transported?
- What are the roles of tropospheric ozone and aerosols in climate change?
- What are the causes of surface UV-B change?

2.4 OMI Description

2.4.1 Main Elements

OMI is composed of the following elements (graphically presented in Figure 1 below):

- Optical Assembly (OA), consisting of the Optical Bench (OPB), two Detector Modules (DEMs), and thermal hardware
- Electronics Unit (ELU), performing CCD readout control and analogue-to-digital conversion
- Interface Adaptor Module (IAM), performing Command Buffering as well as the Data Formatting and Satellite Bus Interface functions

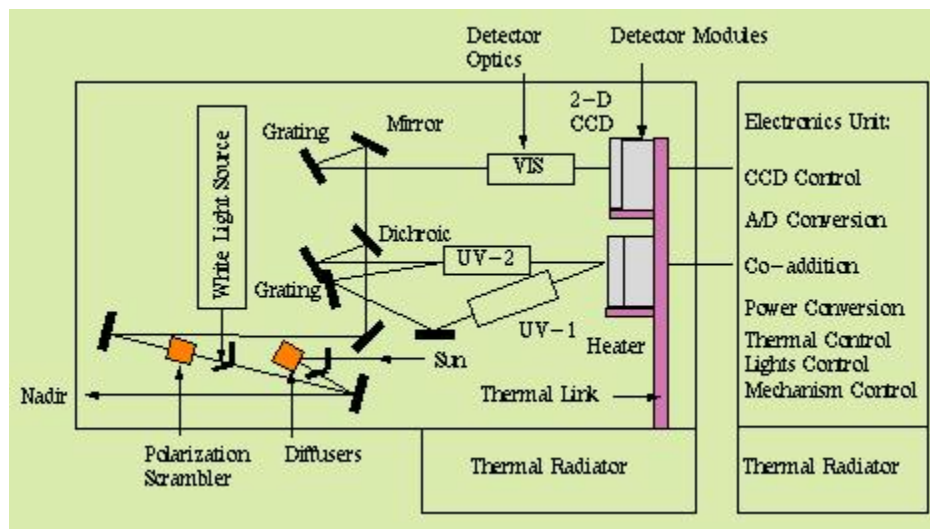


Figure 1: OMI Description

You can find a detailed OMI description at

http://www.knmi.nl/omi/documents/data/OMI_ATBD_Volume_1_V1d1.pdf

or at

http://www.knmi.nl/omi/documents/data/IEEE_OMI-Calibration_May2006.pdf



Table 1: General Description of OMI

Parameter	Value
Wavelength Range:	UV-1: 264-311 nm UV-2: 307-383 nm VIS: 349-504 nm
Spectral Resolution (FWHM):	UV-1: 0.63 nm UV-2: 0.42 nm VIS: 0.63 nm
Spectral Sampling (FWHM):	UV-1: 1.9 px UV-2: 3.0 px VIS: 3.0 px
Telescope FOV:	115° (2600 km on ground)
IFOV:	12 km × 6 km (flight direction × cross-flight direction)
Detector:	CCD: 780 × 576 (spectral × spatial) pixels
Mass:	65 kg
Duty Cycle:	60 minutes on daylight side 10-30 minutes on eclipse side (calibration)
Power:	66 watts
Data Rate:	0.8 Mbps (average)

2.4.2 Measurement Principle

OMI is a wide-angle, non-scanning and nadir-viewing instrument measuring the solar backscattered irradiance in a swath of 2600 km. The telescope Field of View (FOV) is 115° wide in across-track dimension. The instrument is designed as a compact UV/VIS imaging spectrograph, using a two-dimensional CCD array for simultaneous spatial and spectral registration (hyperspectral imaging in frame-transfer mode). The instrument has two channels measuring in the spectral range of 264-504 nm.

OMI employs a polarization scrambler that makes the instrument insensitive to the polarization state of the incoming radiance. The radiation is then focused by the secondary telescope mirror. A dichroic element separates the radiation into a UV and a VIS channel. The UV channel is split again into two subchannels: UV-1 (264-311 nm) and UV-2 (307-383 nm). In the UV-1 subchannel, the spatial sampling distance per pixel is a factor two larger than in the UV-2 subchannel. The idea is to increase the ratio between the useful signal and the dark current signal, and therefore increase the Signal-to-Noise Ratio (SNR) in UV-1, and to suppress the stray light below 300 nm. The resulting Instantaneous Field of View (IFOV) values of a pixel in the cross-track direction are 12 km for UV-1 and 6 km for UV-2 and VIS. Groups of 4 or 8 CCD detector pixels are binned in the cross-track direction.



Five subsequent CCD images, each with a nominal exposure time of 0.4 s., are electronically co-added during a basic 2-second interval (the so-called “master clock period”). This results in an FOV of 13 km in the along-track direction. In addition, one column (wavelength) of each CCD data is downlinked without co-adding (monitoring of clouds, ground albedo). The pixel binning and image co-adding techniques are used to increase SNR and to reduce the data rate.

Images in the UV-1 channel have a 30-pixel resolution in the full cross-track direction, while those in the UV-2 and VIS channels have 60 pixels for the same full width. Details of these channels are provided in Table 2. For all the channels, the one-dimensional cross-track image is roughly perpendicular to the ground track and covers a distance of 2600 km on the earth's surface.

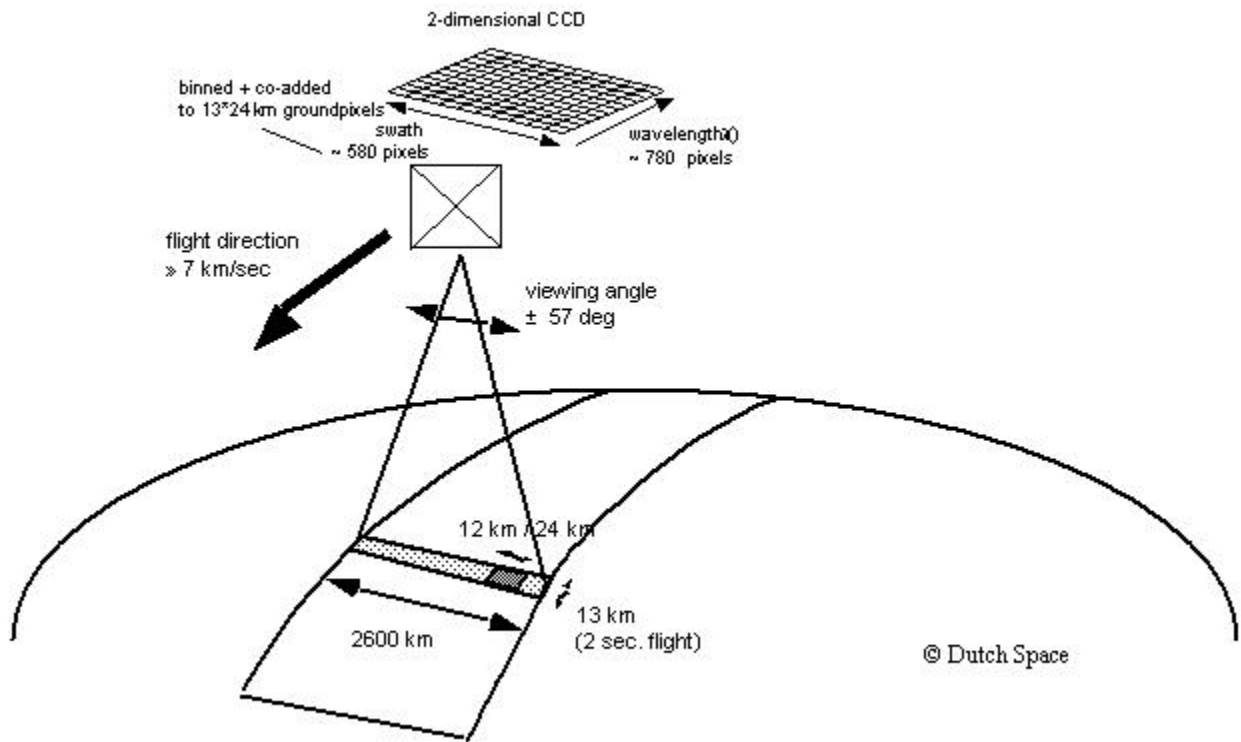


Figure 2: OMI Measurement Design



2.4.3 Observation Modes

OMI works in three different modes:

- Global mode
- Spatial zoom-in mode
- Spectral zoom-in mode

The global measurement mode is the default mode, sampling the complete swath of 2600 km for the complete wavelength range. The ground pixel size at nadir position in the global mode is $13 \times 24 \text{ km}^2$ (along-track \times cross-track) for the UV-2 and VIS channels, and $13 \times 48 \text{ km}^2$ for the UV-1 channel.

The spatial zoom-in mode has a nadir ground pixel size of $13 \times 12 \text{ km}^2$, but the swath width has a minimum of 725 km. The spatial zoom-in mode is used one day each 32 days, always above the same geo-locations. In the spectral range of 264-311 nm, the pixel size in the cross-track direction is twice as large (that is, a nadir ground pixel size of $13 \times 24 \text{ km}^2$). The swath is symmetric with respect to the sub-satellite track. The spatial zoom-in mode results in two products:

- A Zoom Radiance product consisting of all the zoom data
- A Global Radiance product in which the zoom data are effectively degraded to match the resolution of images produced in the global mode but only cover half the normal mode radiance.

The spectral zoom-in mode has a nadir ground pixel size of $13 \times 12 \text{ km}^2$ and a full swath of 2600 km. It has a limited spectral coverage of 307-432 nm to cover the most important scientific products. This mode was tested during the pre-launch period and run a few times between early August and early October 2004, during Launch and Early Operations (LEO). Because this mode has not been used since that time, it is not addressed in this document.

In Figure 3 below, the narrower swaths on the left-hand side of the image demonstrate retrievals from spatial zoom-in mode radiance measurements.

OMDOAO3 Total Column Ozone on 2007-02-27 for Orbits 13932-13946

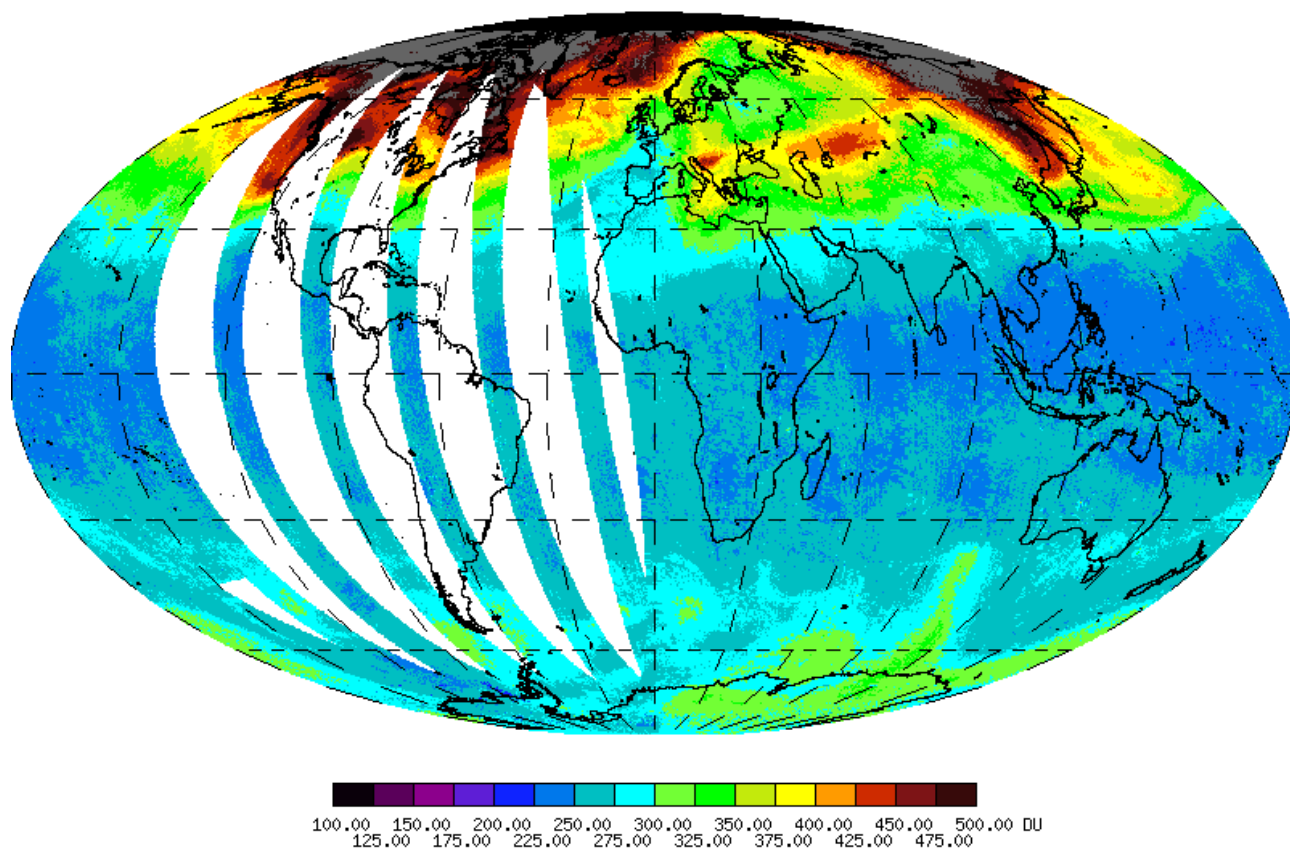


Figure 3: An Image of DOAS O₃ Product (OMDOAO3).



Table 2: Spectral Range, Resolution and Sampling Distances

Channel	Full Performance Range	Average Spectral Resolution (FWHM)	Average Spectral Sampling Distance
UV-1	264 – 311 nm	0.63 nm	0.33 nm/pixel
UV-2	307 – 383 nm	0.42 nm	0.14 nm/pixel
VIS	349 – 504 nm	0.63 nm	0.21 nm/pixel

Table 3: Characteristics of the Main Observation Modes

Observation Mode	Spectral Range	Swath Width Range	Ground Pixel Size at Nadir	Application
Global Mode				
UV-1	264 – 311 nm	2600 km	13 × 48 km ²	Global observation of all products
UV-2 & VIS	307-504 nm	2600 km	13 × 24 km ²	
Spatial Zoom-in Mode				
UV-1	264 – 311 nm	2600 km	13 × 24 km ²	Regional studies of all products
UV-2 & VIS	307-504 nm	725 km	13 × 12 km ²	



Chapter 3: OMI Data Products

3.1 OMI Data Processing and Product Summary

OMI data are processed at the OMI Science Investigator-led Processing System (SIPS) Facility in Greenbelt, Maryland, and are archived at the NASA Goddard Earth Sciences Data and Information Services Center (GES DISC). The OMI data products are available at four processing levels: Level 0, Level 1B, Level 2, and Level 3.

Level 0 products are raw sensor counts. Level 0 data are packaged into two-hour “chunks” of observations in the life of the spacecraft (and the OMI aboard it) irrespective of orbital boundaries. Level 1B processing takes Level 0 data and calibrates, geo-locates and packages the data into orbits.

Level 0, Level 1B, and Level 2 products contain orbital swath data, whereas Level 3 products contain global data that are composited over time (daily or monthly) or over space for small equal angle (latitude \times longitude) grids covering the whole globe. The OMI data are implemented in the following 4 levels:

- Level 1B
- Level 2
- Level 2G
- Level 3

OMI Level 2 data files also contain temporal, spatial, solar, and viewing geometry parameters, quality flags, and extensive quality assurance information, in addition to the standard retrieved geophysical parameters. Sections 3.2 through 3.4 describe Standard Products. Section 3.5 describes existing Level 3 Special Products.

3.2 Level 1B Products: OMI Radiometrically Calibrated and Geo-located Radiance Products

The extensive calibration and data processing algorithm Ground Data Processing System (GDPS), was developed by Dutch Space in cooperation with the Dutch OMI team (Torres et al., 2007; Torres et al., 2008; van den Oord et al., 2002; van den Oord et al., 2006). The Level 0 to 1B algorithm is used at OSIPS (NASA GSFC) to produce Level 1B OMI products. This algorithm takes the raw sensor measurements (Level 0 data), calibration, and spacecraft attitude and ephemeris information to produce radiometrically calibrated and geo-located radiances. There are six types of Level 1B Standard Products as shown in Table 4.



The lead scientist for Level 1B products is M. Dobber (dobber@knmi.nl). The calibration website <http://www.knmi.nl/omi/research/calibration> publishes extensive daily reports and anomaly reports.

For more information about available Level 1B products, refer to the Aura Validation Data Center's OMI Data page at: <http://avdc.gsfc.nasa.gov/Data/Aura/OMI/OM1B/index.html>

Table 4. OMI Calibrated and Geo-located Earth View Radiance, Solar Irradiance, and Calibration Products (Level 1B)

OMI Level 1B Calibrated Radiance & Irradiance (Orbital)	
Product	Product Description
OML1BRUG	<i>Geo-located Earth View UV Radiance, Global-Mode Product</i> Geo-located earth view radiances from the UV channel detector in the wavelength range of 264-383 nm, using the global measurement mode. It also contains the data re-binned from the observations taken using zoom-in measurement modes.
OML1BRVG	<i>Geo-located Earth View VIS Radiance, Global-Mode Product</i> Geo-located earth view radiances from the VIS channel detector in the wavelength range of 349-504 nm, using the global measurement mode. It also contains the data re-binned from the observations taken using zoom-in measurement modes.
OML1BRUZ	<i>Geo-located Earth View UV Radiance, Zoom-in Mode Product</i> Geo-located earth view radiances from the UV channel detector in the wavelength range of 264-383 nm, using spectral and spatial zoom-in measurement modes.
OML1BRVZ	<i>Geo-located Earth View VIS Radiance, Zoom-in Mode Product</i> Geo-located earth view radiances from the VIS channel detector in the wavelength range of 349-504 nm, using spectral and spatial zoom-in measurement modes.
OML1BIRR	<i>Solar Irradiance Product</i> Averaged sun measurements of the solar irradiances from both the UV and VIS channel detectors over a single solar observation in the wavelength range of 264-504 nm. Contains solar measurement data products for both the global and the spatial zoom-in mode. This product only contains measurement data obtained with the quartz volume diffuser.
OML1BCAL	<i>Calibration Data</i> In-flight calibration measurement results, including the complete CCD readouts for both the UV and VIS channels from the areas on the CCD that are intended for calibration purposes (which is outside of the area normally used by the spectrometer). All White Light Source (WLS) and LED measurements are also stored in this product. Solar measurement data from all three on-board diffusers is stored in the calibration data product.



3.3 Level 2 Products: OMI Orbital Atmospheric Products

The OMI Level 2 (orbital swaths) products contain the geophysical parameters (at ground-pixel resolution) derived from radiometrically calibrated and geo-located radiances (Level 1B product). Refer to Table 5 below for the spectral radiances used for the retrieval of OMI products.

Each Level 2 product file consists of parameters retrieved from observations made only in the daytime portion of an orbit (~ 53-minute duration). In addition to standard derived parameters, these files also contain some auxiliary derived parameters, ancillary input parameters, temporal, spatial, solar and viewing geometry, terrain height, ground-pixel quality flags, and extensive quality assurance information. In the OMI global operational mode, the spatial resolution is 13 × 24 km² at nadir.

Almost all Level 2 products contain data at 13 × 24 km² (nadir pixel size) resolution with the exception of zoom-in products and the ozone profile product. Level 2 products are available at higher spatial resolution using the OMI spatial zoom-in mode data at 13 × 12 km² resolution. These products' short names end with a Z (for zoom-in). The ozone profile product will be available with a spatial resolution of 13 × 48 km².

Table 5. OMI Level 2 Product Description

Product Description	Acronym	Spectral Range (nm)	Release Dates	Granule File Size in (MB)
Surface spectral irradiance & Erythemally weighted UV Flux	OMUVB	305, 310, 324, 380	April 20, 2007	8.5
Ozone column: DOAS method	OMDOAO3	331.1-336.1	June 26, 2006	11
Ozone column: TOMS Version 8 method	OMTO3	317.5, 331.2, 360	April 29, 2005	48
Aerosol: near-UV algorithm	OMAERUV	354-388	August 31, 2006	6
Aerosol: multi-wavelength algorithm	OMAERO	331-500	March 22, 2007 (Provisional)	12
Cloud Fraction and Cloud Pressure: O ₂ -O ₂ absorption method	OMCLDO2	477	June 26, 2006	15
Cloud Fraction and Cloud Pressure: Rotational Raman method	OMCLDRR	346-354	April 20, 2006	6



Product Description	Acronym	Spectral Range (nm)	Release Dates	Granule File Size in (MB)
O ₃ Profile	OMPROO3	270-340	March 2007 (Provisional)	30
SO ₂	OMSO2	310.8-314.4 345-370	December 20, 2006	21
HCHO	OMHCHO	325-357	February 1, 2007	5
BrO	OMBRO	338-357	February 1, 2007	5
OCIO	OMOCLO	366-401	February 1, 2007	5
NO ₂	OMNO2	405-465	September 29, 2006	17

Level 2 products consist of the products in the different categories:

- Ozone products
- Clouds, Aerosols and Surface UV Irradiance products
- Trace Gases products

3.3.1 Ozone Products

There are three Level 2 (L2) ozone products based on the algorithms that originated from the Total Ozone Mapping Spectrometer (TOMS), the Global Ozone Monitoring Experiment (GOME), and the Scanning Imaging Absorption Spectrometer for Atmospheric CHartographY (SCIAMACHY). These ozone products provide column ozone and ozone profiles.

Two algorithms are available for the total ozone retrieval: the enhanced TOMS Version 8 (V8) algorithm used to process all 25 years of TOMS data and the Differential Optical Absorption Spectroscopy (DOAS) technique used with GOME and SCIAMACHY ozone retrievals. The TOMS V8 algorithm retrieves vertical column ozone data essentially using 317.5 and 331.2 nm wavelengths (Ahn et al., 2008; Bhartia and Wellemeyer, 2002). OMI's additional hyperspectral measurements provide better estimates and corrections of the factors that induce uncertainty in ozone retrieval (for example, cloud and aerosol, sea-glint effects, profile shape sensitivity, SO₂ and other trace gas contamination). The DOAS technique is based on the fitting of the satellite-measured gases absorption structure at the number of absorption lines in the spectral region 331.1-336 nm to the gases absorption structure measured in the laboratory (Veefkind, J.P., and J.F. de Haan, 2002; Veefkind et al., 2006). Slant column density is determined first and then is translated into vertical column density using an air mass factor, which is computed using radiative transfer models.



Table 6. OMI Ozone Products (Level 2)

OMI Ozone (Total column & Profile)		
Product	Parameters	Lead Scientist
OMTO3	O ₃ total column (TOMS V8 method), also other derived and ancillary parameters including N-values, effective Lambertian scene-reflectivity, UV aerosol index, SO ₂ index, cloud fraction, terrain and cloud pressure, ozone below clouds, geo-location, solar and satellite viewing angles, and quality flags.	P.K. Bhartia Pawan.K.Bhartia@nasa.gov
OMDOAO3	O ₃ total column (DOAS method), ozone slant column density and its precision (for data assimilation), also other derived and ancillary parameters including ozone ghost column density, air mass factor (all, clear, and cloudy scenes), scene reflectivity, radiance over the DOAS fit window (331.1 to 336.1 nm), root mean square of DOAS fit, cloud fraction, cloud radiance, terrain and cloud pressure, geo-location, viewing angles, and quality flags.	J.P. Veefkind veefkind@knmi.nl
OMPROO3	O ₃ profile (optimum estimation method), as well as a priori profile (including uncertainties) for 17 layers, correlation coefficients, averaging kernel, root mean square of fit, total ozone (obtained by integrating the profile), geo-location, solar and satellite viewing angles, and quality flags. This product comes from the Royal Meteorological Institute (Dutch: <i>Koninklijk Nederlands Meteorologisch Instituut</i> , KNMI) and will be archived at the NASA GES DISC as a standard product.	J.F. de Haan haandej@knmi.nl

Ozone profile retrieval is based on the Optimal Estimation method (also referred to as Rodger's maximum-likelihood estimation technique), uses all ozone sensitive wavelengths' radiances (in spectral region 270 to 340 nm), a priori ozone profile, radiances, and a Jacobian matrix computed from the radiative transfer model (van Oss et al., 2002). Hyperspectral capabilities provide better vertical resolution below 20 km compared to the Solar Backscatter Ultraviolet instrument (SBUV), which has 12 wavelengths, not all of which are used to determine profile ozone.

3.3.2 Clouds, Aerosols and Surface UV Irradiance Products

OMI produces cloud fraction and cloud pressure measurements that are used in OMI trace-gas retrievals and in the retrieval of data products from other Aura sensors. The two methods used for the cloud pressure retrieval are the O₂-O₂ absorption method and the Rotational Raman Scattering (RRS) method. The O₂-O₂ absorption method is based on spectral fitting of O₂-O₂ absorption band at 477 nm using the Differential Optical



Absorption Spectroscopy (DOAS) technique (Acarreta and de Haan, 2002; KNMI website: <http://www.knmi.nl/omi/research/documents/>). The RRS method is based on the least square fitting of the ring spectrum (Joiner, et al., 2002; 2006; Vasilkov et al., 2004).

Users should be aware that both the cloud pressure and fraction derived from both OMI algorithms are effective, meaning that the cloud fraction may not represent true geometrical cloud fraction and that cloud pressure may not represent a true cloud top pressure.

The cloud fraction is determined such that the average top of atmosphere reflectance over the fit window is reproduced with a Lambertian reflector. The pressure of this Lambertian cloud is adjusted to reproduce the intensity of the pressure sensitive feature (the depth of the O₂-O₂ absorption near 475 nm or the amount of filling in of the Fraunhofer lines in the solar spectrum by rotational Raman scattering). Model studies and limited comparisons with CloudSat have shown that this pressure level is generally well within the cloud.

OMI also provides aerosol information needed by other Aura algorithms. Two algorithms (near-UV and multi-wavelength methods) are used for the retrieval of aerosol characteristics over the ocean and land (Torres et al., 2002). The availability of the near-UV wavelengths also makes the aerosol retrieval over the desert area possible since the land reflectance is small at these wavelengths. In addition to providing information on the aerosol absorption and single scattering albedo, OMI aerosol algorithms can differentiate between sulfate, smoke and dust aerosols, and characterize the type of urban aerosols. The aerosol index (a side product of the near-UV method) is used for detection of absorbing aerosols even in cloudy scenes and above snow/ice surfaces.

The spectral surface irradiance (at 305, 310, 324, and 380 nm) reaching the ground and erythemally weighted irradiance (covering 290-400 nm) are produced using the enhanced version of TOMS Surface UV-B flux algorithm (Krotkov et al., 2002; , Krotkov et al., 2006).

Measured earth-atmosphere radiances are used in conjunction with the radiative transfer model to retrieve UV spectral irradiances reaching the ground. The OMI algorithm uses actual snow thickness information from the European Centre for Medium-Range Weather Forecasts (ECMWF) analysis, which improves the accuracy of the values for the high latitudes.

The erythemal UV exposure is calculated using a model for the susceptibility of Caucasian skin to sunburn (erythemal). Table 7 also provides some highlights of clouds, aerosols and surface irradiance exposure products.



Table 7. OMI Clouds, Aerosols, and Surface UV Exposure Products (Level 2)

Clouds		
Product	Parameters	Lead Scientist
OMCLDO2	Cloud fraction and cloud pressure (O ₂ -O ₂ absorption method), slant column O ₂ -O ₂ and O ₃ , ring coefficients, and uncertainties in derived parameters, terrain and geo-location information, solar and satellite viewing angles, and quality flags.	J.F. de Haan haandej@knmi.nl
OMCLDRR	Cloud fraction and cloud pressure (Rotational Raman scattering method), other derived and ancillary parameters, terrain and geo-location information, solar and satellite viewing angles, and quality flags.	J. Joiner Joanna.Joiner-1@nasa.gov
Aerosols over Ocean and Land		
OMAERO	Aerosol characteristics such as aerosol optical thickness, aerosol indices, aerosol type, as well as ancillary information. The aerosol type gives an indication about the single scattering albedo, the layer height, and the size distribution.	B. Veihelmann veihelman@knmi.nl
OMAERUV	UV aerosol index (UVAI), aerosol extinction optical depth (AOD), and aerosol absorption optical depth (AAOD).	O. Torres Omar.Torres.1@gsfc.nasa.gov
Surface UV-Irradiance		
OMUVB	Surface erythemal UV exposure (TOMS algorithm): downward spectral irradiances (W/m ² /nm) at the ground for 305, 310, 324, and 380 nm; erythemally weighted UV irradiance (W/m ²) covering 290-400 nm spectral region (noontime values and daily averages). This product is produced at FMI (Finland), and is archived at NASA GES DISC as a standard product.	A. Tanskanen Aapo.tanskanen@fmi.fi



3.3.3 Trace Gases Products

Total column and slant column values of trace gases, NO₂, BrO, HCHO, OCIO, and SO₂ are produced by fitting absorption spectra. (Chance et al., 2002; Boersma et al., 2002; Krotkov et al., 2007; Krotkov et al., 2008; Krueger et al., 2002). Table 8 provides highlights of these products. The OMI algorithm detects volcanic ash and sulfur dioxide produced in volcanic eruptions with up to 40 times more sensitivity than TOMS and GOME (Krueger et al., 2002).

Table 8. OMI Trace Gases Products (Level 2)

Trace Gases (NO₂, BrO, HCHO, OCIO, and SO₂)		
Product	Parameters	Lead Scientist
OMNO ₂	NO ₂ total and tropospheric column, slant column density, one sigma fitting uncertainties for the NO ₂ and the other species varied in the fitting window, correlation of other fitted species to the NO ₂ , fitting root mean square (rms), surface reflectivity, cloud top height, geo-location, and solar and satellite viewing angles.	J. Gleason James.F.Gleason@nasa.gov J.P. Veefkind veefkind@knmi.nl
OMBRO	BrO total column and slant column abundance, one sigma fitting uncertainties for the BrO and the other species varied in the fitting window, correlation of other fitted species to the BrO, fitting RMS, surface reflectivity, cloud top height, quality flags, geo-location, and solar and satellite viewing angles.	K. Chance kchance@cfa.harvard.edu
OMHCHO	HCHO total column and slant column abundance, one sigma fitting uncertainties for the HCHO and the other species varied in the fitting window, correlation of other fitted species to the HCHO, fitting RMS, surface reflectivity, cloud top height, quality flags, geo-location, and solar and satellite viewing angles.	K. Chance kchance@cfa.harvard.edu
OMOCLO	OCIO slant column and one sigma fitting uncertainties for the OCIO and the other species varied in the fitting window, correlation of other fitted species to the OCIO, fitting RMS, surface reflectivity, cloud top height, quality flags, geo-location, and solar and satellite viewing angles. Note that this product is not global (retrieved for polar regions only).	K. Chance kchance@cfa.harvard.edu
OMSO ₂	Total SO ₂ (vertical column in Dobson Units, where 1DU=2.69 × 10 ¹⁶ molecules/cm ²), adjustments to OMT03 total ozone and Lambertian equivalent UV reflectivity, Effective cloud pressure, and ancillary information (satellite geometry, quality flags, geo-location).	N. Krotkov Nickolay.A.Krotkov@nasa.gov



3.4 Level 2G Products

Level 2G (L2G) datasets contain one day's worth of the Level 2 data (typically 14 orbits) ordered by ground position rather than by time. Only the most relevant L2 fields are included in the L2G. In an L2G dataset, each of the pixels from the included L2 files is assigned to a point on a $\frac{1}{4}$ by $\frac{1}{4}$ degree latitude/longitude grid. By precise definition, however, this is not a gridded product because pixels from different L2 datasets are not combined in any way; that is, all L2 pixels are included in the dataset. The transformation into a L2G dataset is reversible (able to be taken back to L2 data) because there is sufficient information stored in the L2G dataset to reproduce the L2 data used to generate it.

L2G datasets are often smaller than the sum of the parts, due in part to data fields that have been dropped, but also due to more efficient use of internal Hierarchical Data Format (HDF5) compression. Users do not need to take any extra steps to use datasets to which internal HDF5 compression has been applied.

The L2G datasets offer a number of benefits, specifically:

- They require equal or less storage space than the 14 or so L2 files used to generate them.
- They reduce by a factor of 14 the number of files in your directories when storing one or more days' worth of consecutive data.
- They reduce by a factor of 14 the number of files your analysis code needs to open when processing one or more days' worth of consecutive data.
- They facilitate gridded (Level 3) product generation.
- They facilitate geographic subsetting.

L2G products have not been generated or released for all L2 standard products. As of the release date of this Guide, L2G products are available for OMI Cloud properties (OMCLDO2G and OMCLDRRG), Ozone Total Column (OMTO3G and OMDOAO3G), Nitrogen Dioxide Total and Tropospheric Columns (OMNO2G), Sulfur Dioxide Total Column (OMSO2G) and Aerosols (OMAERUVG).



3.5 Level 3 Products: OMI Global Gridded Atmospheric Products

Each Level 2 product file contains data from a single orbit. For each Level 2 product there are 14 files per day. OMI Level 3 daily global products are produced by averaging data over small equal angle grids (0.25 degree \times 0.25 degree), (0.5 degree \times 0.5 degree) or (1 degree \times 1 degree) covering the whole globe. Each grid also contains the corresponding statistical parameters (number of pixels, minimum, maximum, and standard deviation).

OMI Level 3 data products of total column ozone and reflectivity can be produced by applying the TOMS Version 8 algorithm to OMI global mode measurements. They are provided on a (1 degree \times 1.25 degree) (latitude by longitude) grid size globally each day.

At the time of this printing, there is only one Level 3 product available (OMUVBL3). In future, a limited number of special products may become L3 products, for example, OMTO3 products and specifications.

For more information on OMUVBL3, refer to <http://disc.gsfc.nasa.gov/Aura/OMI/omuvbl3.shtml>.



Chapter 4: Quality Assessment of OMI Level 2 Products

Currently, OMBRO, OMHCHO, and OMOClo are available as Version 2 products. All other products are available as Version 3 products. All users should use Version 3 products if they are available.

NOTE: Collection 2 for Level 1B products represents the best pre-launch calibration, and Collection 3 for Level 1B products represents the best post-launch calibration. Version 2 products are obtained from Collection 2, and Version 3 products are obtained from Collection 3.

4.1 OMI Pixel Size

Understanding pixel shape and size is an important aspect of assessing the quality of data products. A single Level 2 product file contains all OMI measurements on the sunlit portion of the Earth, for a single Aura orbit. During one orbit, OMI performs approximately 1650 measurements, which take 2 seconds each. In the global observation mode, 60 cross-track ground pixels are measured simultaneously during each measurement. These 60 measurements cover a swath approximately 2600 km wide.

Figure 4 shows the pixel size and orientation across the scan for the two UV channels. Due to curvature of the Earth and the slight asymmetric alignment between the instrument's optical axis and the spacecraft axes, the ground pixels are not symmetrically aligned with respect to the orbital plane. (Note that the latitude and longitude cover different distances on the Earth's surface.) The satellite trajectory in this figure is in the direction of increasing latitude.

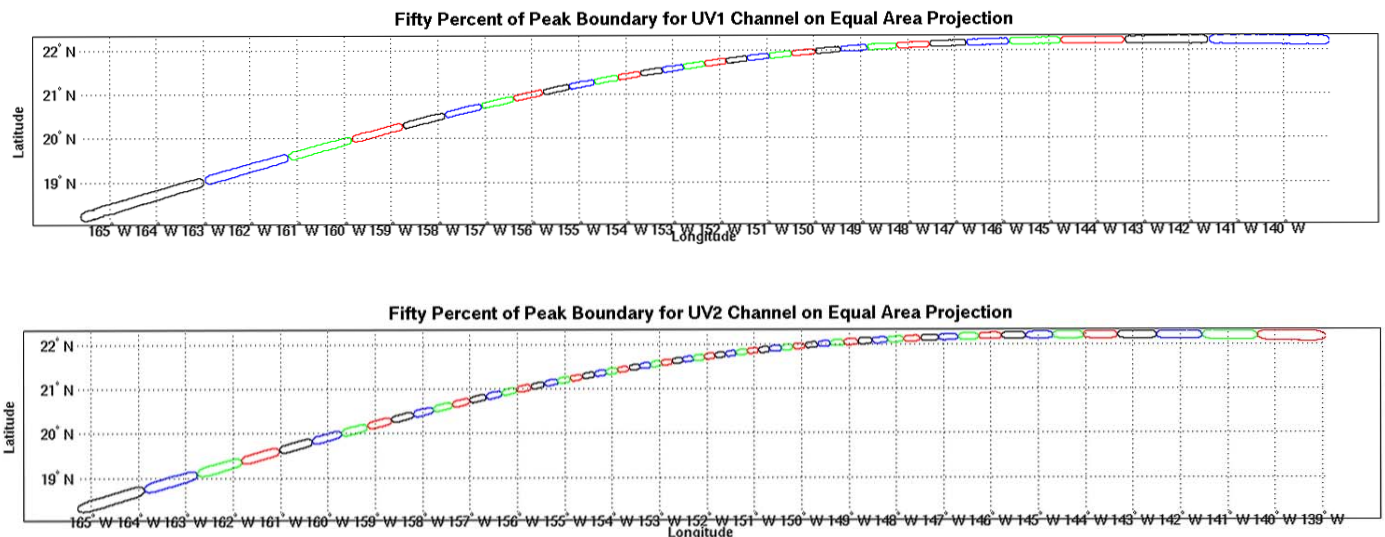


Figure 4: The Position of 60 Ground Pixels for an OMI Measurement



The following pixel dimensions and sizes were computed at the Earth's surface on the WGS84 ellipsoid.

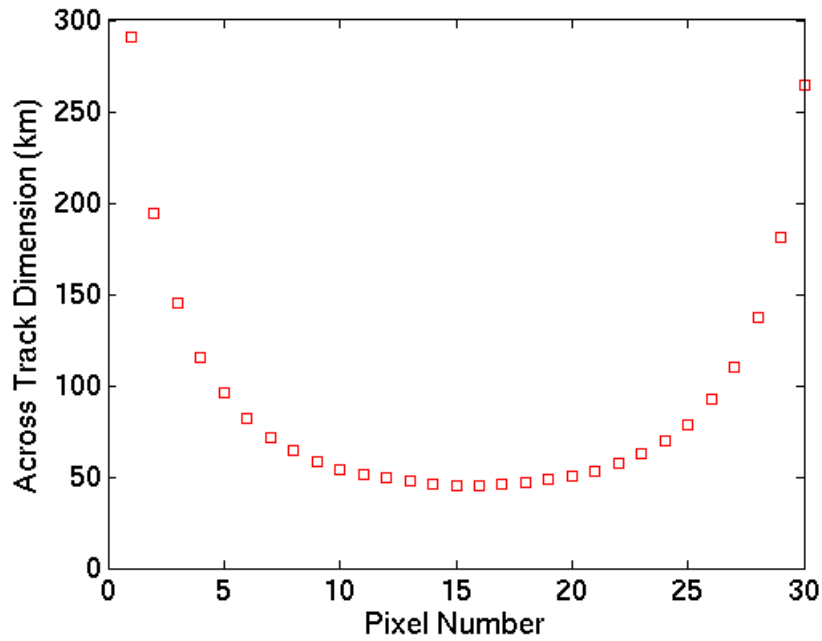


Figure 5: UV1 Cross-Track Dimension Versus Scan Position

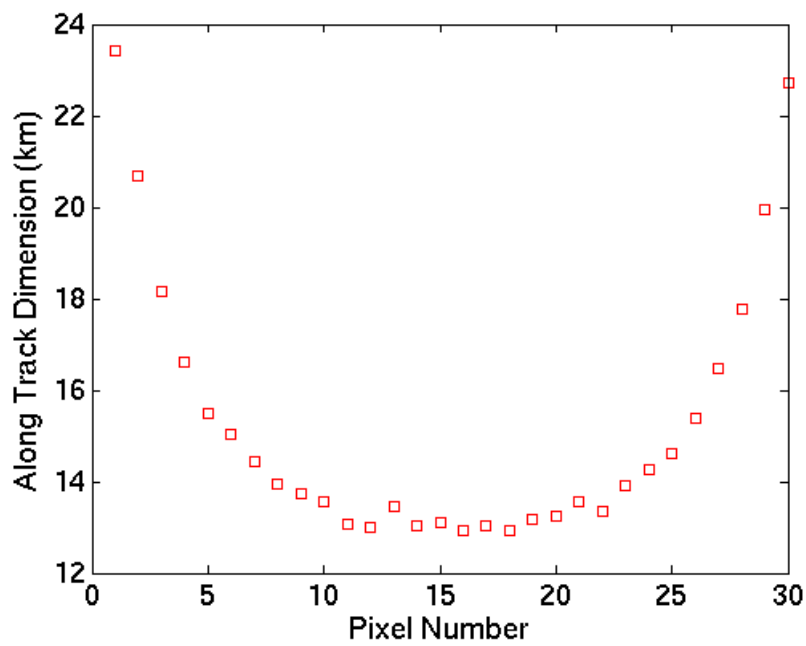


Figure 6: UV1 Along-Track Dimension Versus Scan Position

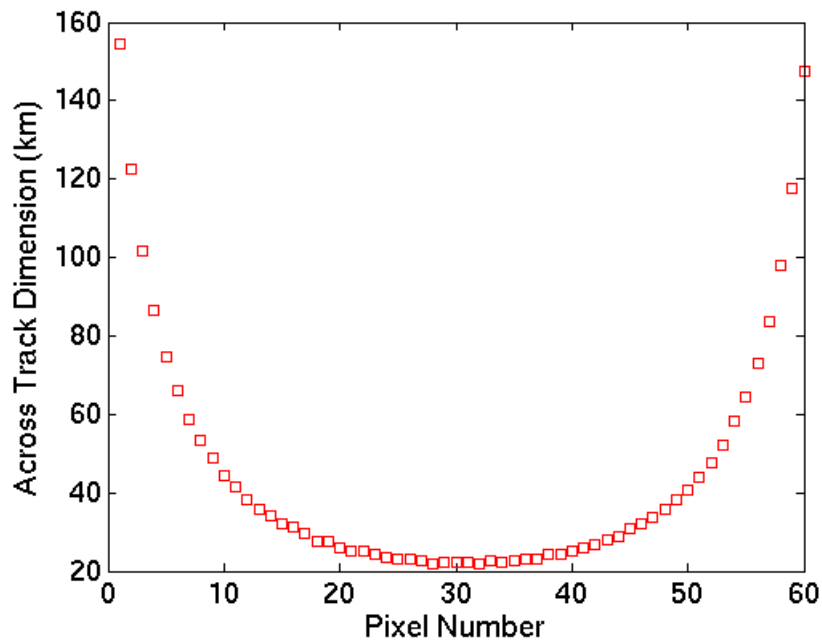


Figure 7: UV2 Cross-Track Dimension Versus Scan Position

Note: The above and below pixel representations show UV2, but the graphs of UV2 and VIS are virtually identical.

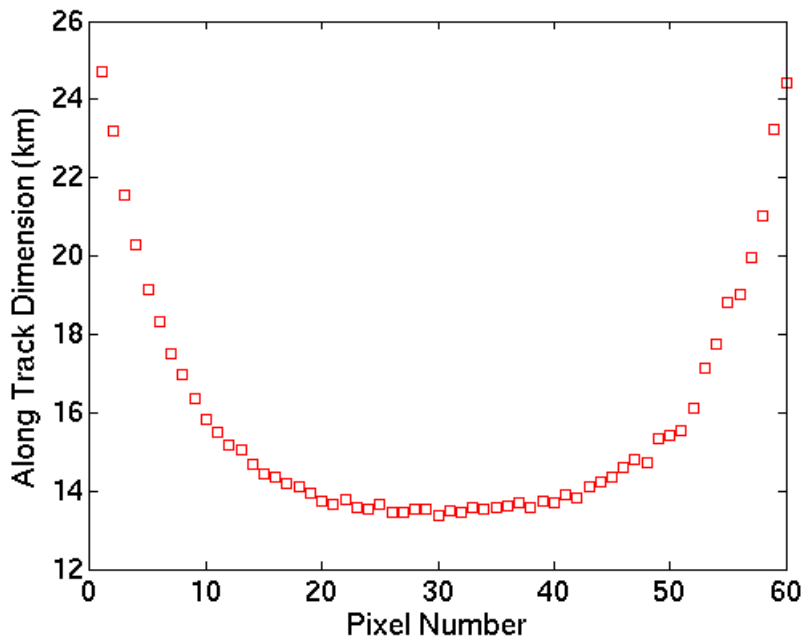


Figure 8: UV2 Along-Track Dimension Versus Scan Position



The following table shows the pixel size at the different scan locations:

Table 9: Pixel Size at Different Scan Locations

<i>Scan Position</i>	<i>UV1 Pixel Size (km²)</i>	<i>UV2 Pixel Size (km²)</i>	<i>VIS Pixel Size (km²)</i>
1	7062.2	3799.4	3800.6
2	4152.2	2803.2	2806.7
3	2775	2168.3	2171.8
4	2040.9	1742	1738.5
5	1586.7	1432.1	1430.9
6	1302.8	1207.9	1209
7	1105.3	1034.1	1036.4
8	968.34	908.16	903.52
9	869.7	803.36	799.89
10	793.16	716.13	719.59
11	742.07	650.99	652.14
12	703.72	596.37	598.67
13	687.27	551.06	548.75
14	661.69	515.04	515.04
15	649.9	480.24	481.38
16	647.32	452.39	448.93
17	659.64	429.18	430.32
18	671.98	402.55	406
19	694.61	392.05	389.75
20	730.97	371.22	373.52
21	778.76	358.46	360.75
22	840.25	356.05	354.89
23	931.43	342.16	346.75
24	1061.4	335.17	335.17
25	1233.7	329.34	328.19
26	1496.1	323.51	326.95
27	1899	317.7	321.14
28	2556.4	317.62	316.47
29	3736.8	317.54	317.54
30	6170.2	310.59	307.15
31		316.25	313.96
32		313.89	312.74
33		321.84	320.69
34		318.34	316.05
35		324	321.71
36		331.95	331.94



<i>Scan Position</i>	<i>UV1 Pixel Size (km²)</i>	<i>UV2 Pixel Size (km²)</i>	<i>VIS Pixel Size (km²)</i>
37		331.89	335.31
38		339.83	339.83
39		350.07	347.77
40		355.73	356.87
41		372.82	372.81
42		381.9	384.19
43		404.71	404.71
44		418.37	421.79
45		448.02	446.87
46		470.81	471.95
47		503.89	505.03
48		533.53	539.24
49		584.88	581.45
50		635.08	629.36
51		687.56	697.83
52		772.01	777.71
53		880.44	870.15
54		1011.7	1012.8
55		1183	1181.8
56		1378.2	1401
57		1654.5	1655.6
58		2047.3	2046.2
59		2652.7	2641.2
60		3554.1	3562

In Figure 9 below, the plot of the 50% power response curve is plotted in black.

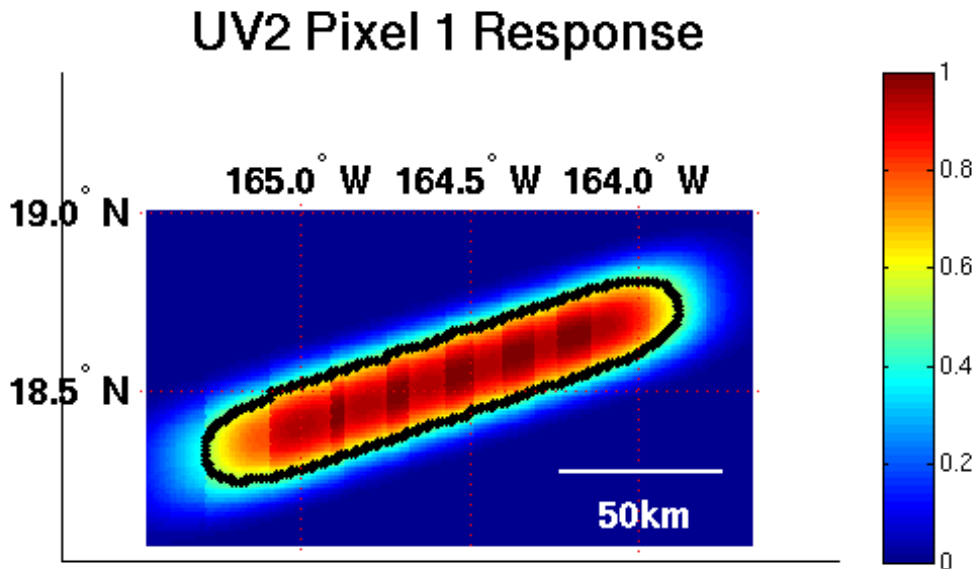


Figure 9: Approximation of Pixel Shape

During zoom-in measurements, the swath width may be reduced. The operational baseline includes zoom-in measurements for one day a month. With zoom-in measurements, 30 of the 60 cross-track pixels contain data; the other 30 contain fill values.

Each Level 2 file contains data from the day lit portion of an orbit (~53 minutes). There are approximately 14 orbits per day. A Level 2 product file is written as an HDF-EOS5 swath file.

Refer to Chapter 3, Table 5, for a summary of the products, and to Tables 6 through 8 for the product descriptions.

Questions related to Level 2 datasets should be directed to the GES DISC (help@disc.gsfc.nasa.gov). You are strongly advised to consult the OMI Quality Assurance Team (omiqa@ltpmail.gsfc.nasa.gov) for most recent information on the assessment of data quality.

4.2 OMI/Aura Aerosol Extinction Optical Depth and Aerosol Types (OMAERO)

4.2.1 Quality Assessment

Various validation studies have been completed or are in progress for the Aerosol Optical Depth (AOD) data from the OMAERO product using ground-based, airborne, and satellite-based observations. Note that the results of current validation studies for land scenes are affected by issues related to the currently used surface albedo climatology. The validation studies for land will be updated and extended once the new surface albedo climatology from OMI data is implemented.



For ocean scenes, global AOD data from the OMAERO product have been compared with measurements from other satellite instruments. Figure 10 below shows such a comparison for the period of June 2006.

The comparison with quality assured data from the MODIS standard product (Figure 10, left side) shows excellent agreement between the datasets. For this comparison, only quality-assured MODIS data (QA flag=3) have been included. By using this data flag, many partly clouded OMI scenes are excluded that are not recognized as being cloudy by the OMI cloud screening scheme. When OMI data are used alone, unrecognized cloud contamination is a significant source of errors. For the comparison with the POLARization and Directionality of the Earth's Reflectances (POLDER) on the Polarization and Anisotropy of Reflectances for Atmospheric Sciences coupled with observations from a Lidar (PARASOL) platform (Figure 10, right side), the data have been filtered based on the quality parameter in the POLDER aerosol algorithm. A correlation coefficient of larger than 0.8 and a regression line slope of 1.07 indicate a good agreement between the datasets.

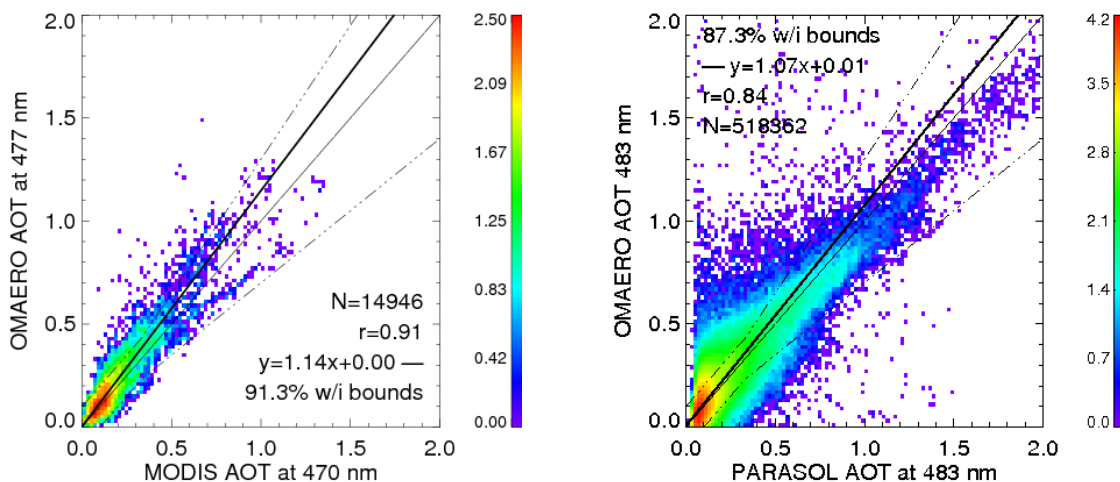


Figure 10: AOD from the OMAERO product compared with quality-assured data from the MODIS standard product (left) and with quality parameter-filtered data from POLDER (right)

For land scenes, we report the results of various validation studies. Curier, et al. (2007) have investigated the AOD data from the OMAERO product for Europe and adjacent oceans. A comparison with MODIS AOD data yields correlation coefficients between 0.76 and 0.81 for ocean, and between 0.59 and 0.70 for land. The difference between land and sea is due to shortcomings in the currently used surface albedo climatology. In the same study, strong site-dependent correlations are reported for comparisons of the AOD from the OMAERO product with ground-based data from various AERONET stations in Europe.

The OMAERO Level 2 product contains diagnostic information about the quality of the fit. Values for the retrieval error of the AOD obtained using the non-linear fitting routine



are mostly below 0.03. This error concerns the AOD retrieval for a given aerosol model and hence does not include error correlations of AOD and microphysical aerosol parameters or the aerosol height. The standard deviation of the AOD values of the aerosol models with a Root Mean Square (RMS) error lower than a given threshold is below 0.11 for 95% of the cases. The standard deviation of the Single Scattering Albedo (SSA) values of the aerosol models with an RMS lower than a given threshold is below 0.1 in 95% of the cases.

4.2.2 Additional Information

Direct questions related to the OMAERO dataset to help-disc@listserv.gsfc.nasa.gov. For questions and comments related to the OMAERO algorithm and data quality, please send an e-mail to omaero@ltpmail.gsfc.nasa.gov.

For more information on this product, refer to:

http://disc.gsfc.nasa.gov/Aura/OMI/omaero_v003.shtml

4.3 OMI/Aura Aerosol Extinction and Absorption Optical Depth (OMAERUV)

4.3.1 Quality Assessment

A very important parameter that is reported in the quality assessment of OMAERUV data is the algorithm quality flag (field name AlgorithmFlags), which contains the processing error flag in its first byte. A detailed description of the data quality flags is given in the OMAERUV readme file http://disc.gsfc.nasa.gov/documents/OMAERUV-README_File_v3.doc. Most users should use data with a data quality flag 0 or 1.

Because of the relatively large footprint of the OMI observations ($13 \times 24 \text{ km}^2$ at nadir), the major factor affecting the quality of aerosol-related products is sub-pixel cloud contamination. Currently, the cloud mask is based on simple reflectivity and UVAI thresholds, which can cause significant overestimation of the mean Aerosol Extinction Optical Depth (AOD). However, experience with TOMS suggests that monthly mean AODs reliably capture variation in the AOD over time. It is important to note, however, that the Aerosol Absorption Optical Depth (AAOD) is less affected by cloud contamination.



In general, OMAERUV retrievals are more reliable over land than over water surfaces. The near-UV retrieval method is particularly sensitive to carbonaceous and mineral aerosols. The sources of these aerosol types are located over the continents, and the atmospheric aerosol load associated with these events is generally large. In addition, dust and smoke aerosol events tend to take place under meteorological conditions that do not favor the formation of clouds near the sources, such as arid and semi-arid areas in the case of dust, and the dry season in the case of biomass burning. The OMAERUV-retrieved AOD of sulfate-based aerosols is less accurate due to its low values, higher spatial variability and increased levels of sub-pixel cloud contamination.

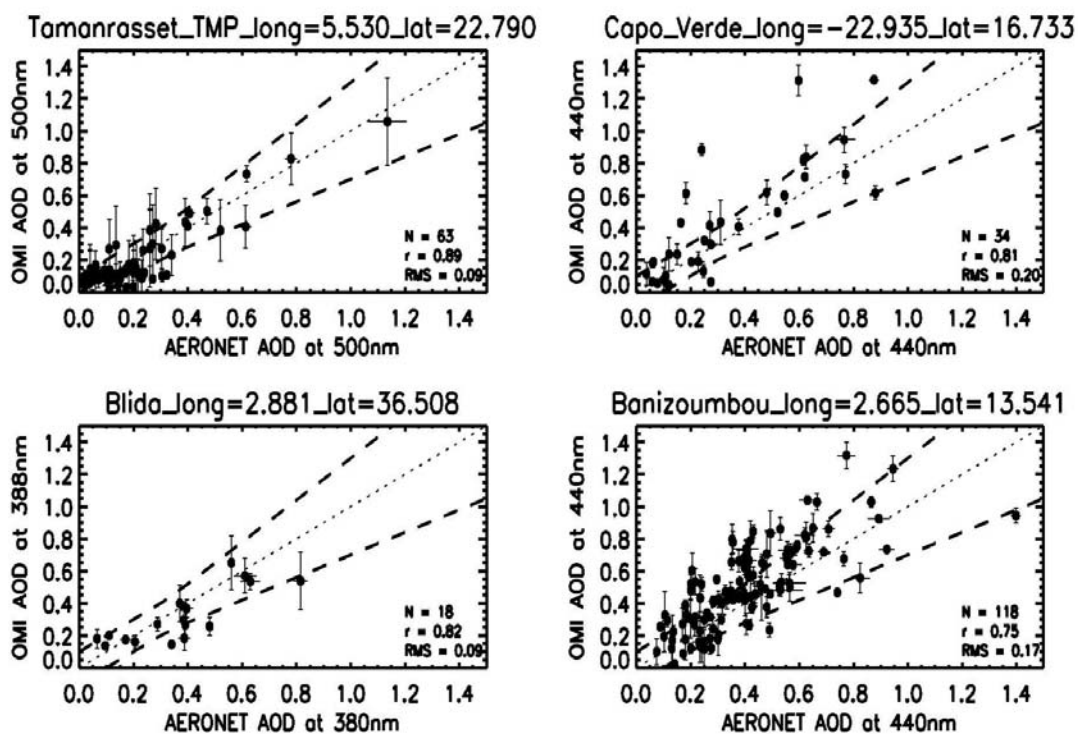


Figure 11. OMAERUV-AERONET comparison over Northern Africa. Retrievals at the Capo-verde and Banizombou sites have been reduced to 440 nm to facilitate the comparison with the ground-based measurements.

Ocean OMAERUV retrievals are affected by other factors. In addition to sub-pixel clouds, the ocean surface reflectance has both angular and spectral variations, the latter due to spectrally varying scattering from the water, often called water-leaving radiances (WLR). Chlorophyll, sediments and other types of suspended matter decrease WLR. Spectral variations of ocean reflectance are accounted for in a climatological sense using a wavelength-dependent surface reflectance dataset. Short-term variability, however, is not taken into account in the current version of the algorithm.



Comparisons of OMAERUV-retrieved extinction optical depth to AERONET observations at several sites show that when cloud-free conditions prevail OMAERUV-observed AOD values are in reasonable agreement with AERONET (Torres et al., 2008). Figure 11 illustrates a comparison of OMAERUV retrieved AOD to AERONET measurements at four Northern Africa sites, where the atmospheric aerosol load typically consists of desert dust. The level of agreement is very good with correlation coefficients between 0.75 and 0.89.

For environments where sub-pixel cloud contamination is persistent during all seasons the statistics of the OMAERUV-AERONET comparisons are poor. For these conditions comparisons over a longer period are needed to better assess the quality of the OMI aerosol product.

As part of the data quality assessment, OMAERUV retrievals of AOD have been compared to MODIS and MISR data for different aerosol types (Ahn et al., 2008). In general, when clear conditions predominate, the OMAERUV retrievals are well correlated with MODIS and MISR AOD products especially for large-scale dust and smoke events. For background aerosol conditions, sub-pixel cloud contamination significantly affects the OMAERUV retrieval.

4.3.2 Additional Information

For questions and comments related to the OMAERUV algorithm and data quality, please contact Omar Torres (omar.torres@hamptonu.edu) who has the overall responsibility for this product.

For more information on this product, refer to http://disc.gsfc.nasa.gov/Aura/OMI/omaeruv_v003.shtml.



4.4 OMI/Aura Bromine Monoxide Total Column (OMBRO)

4.4.1 Quality Assessment

Fitting uncertainties for the BrO slant columns typically range between 25-100 %, with as low as 5 % over BrO hotspots. This is roughly 2-4 times what was achieved from GOME. Uncertainties in the stratospheric Air Mass Factor (AMF) that is used to convert slant to vertical columns are estimated to be 10 % or less. Hence, the total uncertainties of the BrO vertical columns typically range within 27-101 %.

Cross-track striping (systematically elevated or reduced column values at the same cross-track position along the whole track) of the BrO columns is a presently outstanding issue. This is not unique to BrO but affects all OMI data products to a greater or lesser degree. Small absorbers like BrO, HCHO and OCIO, however, are more strongly affected by striping since the column values are of a similar order of magnitude as the stripes, such that the effect is relatively stronger. Various efforts, both at Level 0-1 and 1-2 data processing are underway to improve this situation, including the method of outlier identification in the fitting residual as employed in the BrO fit. A satisfactory solution remains to be found, and users of the BrO columns must be aware of this issue.

The BrO data product provides RMS and one standard deviation (1σ) fitting uncertainties, as derived from the fitting covariance matrix. These uncertainties do not include contributions from uncertainties in the measurements or the reference cross-sections. In addition to the uncertainties, a fitting diagnostic flag (FitConvergenceFlag) provides information on non-convergence of the fitting process. This flag should be consulted for more details on the quality of a particular BrO column datum.



Table 10: Quality Flag Scheme for OMBRO

Value	Classification	Rationale
0	Good	All quality checks passed; data may be used with confidence
1	Suspect	Caution advised because one or more of the following conditions are present: <ul style="list-style-type: none"> • FitConvergence Flag is < 300 (but > 0): convergence at noise level • Column + 1σ uncertainty < 0
2	Bad	Avoid using data because one or more of the following conditions are present: <ul style="list-style-type: none"> • FitConvergenceFlag is < 0: abnormal termination, no convergence • Column + 1σ uncertainty < 0
-1	Missing	No column values have been computed; entries are missing

4.4.2 Additional Information

For questions and comments related to the OMBRO algorithm and data quality, please contact Thomas P. Kurosu (tkurosu@cfa.harvard.edu). Please send a copy of your e-mail to Kelly Chance (kchance@cfa.harvard.edu), who has the overall responsibility for this product.

For more information on this product, refer to

<http://www.cfa.harvard.edu/~tkurosu/SatelliteInstruments/OMI/PGEReleases/index.html>

and

http://www.cfa.harvard.edu/~tkurosu/SatelliteInstruments/OMI/PGEReleases/READMEs/OMBRO_README.pdf



4.5 OMI/Aura Cloud Pressure and Fraction (O_2-O_2 Absorption) (OMCLDO2)

4.5.1 Quality Assessment

The OMCLDO2 effective cloud fraction and cloud pressure have been compared to MODIS-Aqua, which flies 15 minutes in front of OMI-Aura. The most important conclusions are as follows:

- The effective cloud fraction of OMI compares well to MODIS. Large differences may occur on snow and ice surfaces. Also, the OMI cloud fractions are slightly higher for low effective cloud fractions.
- The cloud top pressure derived from MODIS is lower (higher clouds) than OMI. This is expected because MODIS uses the thermal infrared, which is more sensitive to higher clouds. The bias between OMI and MODIS is approximately 100 hPa, with a standard deviation of 200 hPa. It is noted that the comparison of the cloud pressure is difficult because of the different wavelength regions.

Further investigations on the accuracy of the OMCLDO2 product are planned. For example, comparisons to airborne and space-borne LIDARs should provide more information on the accuracy of the derived cloud pressure.

4.5.2 Additional Information

For questions and comments related to the OMCLDO2 algorithm and data quality, please contact omcldo2@ltpmail.gsfc.nasa.gov.

For more information on this product, refer to:
http://disc.gsfc.nasa.gov/Aura/OMI/omcldo2_v003.shtml



4.6 OMI/Aura Cloud Pressure and Fraction (Raman Scattering) (OMCLDRR)

4.6.1 Quality Assessment

When accessing data quality, be aware that both the OMCLDRR cloud pressure and fraction are “effective,” meaning that the cloud fraction does not represent true geometrical cloud fraction and the cloud pressure may not represent the true physical cloud-top pressure (especially in the case of multiple cloud layers). Specifically, it is difficult to derive a sub-pixel cloud fraction using OMI radiances. The effective cloud fraction is based on gross assumptions about the cloud and ground reflectivities. The effective cloud fraction is intended for use in conjunction with the effective cloud pressure such that the combination of the two produces the amount of observed Raman scattering.

The cloud pressures are representative of pressure levels reached by back-scattered photons averaged over a weighting function. The algorithm uses the concept of the Mixed Lambertian-Equivalent Reflectivity (MLER) in which a surface (cloud or ground) is assumed opaque and Lambertian. In the MLER model, a cloud fraction is used to weight the radiances coming from the clear and cloudy portions of the pixel. The algorithm computes an effective cloud fraction using assumptions about the cloud and ground reflectivities as will be described below. Scattering and/or absorption from within and below a cloud or between multiple cloud decks can be accounted for by using a pressure higher than the physical cloud top. The derived effective cloud pressures are therefore typically higher than (that is, lower in altitude) cloud-top pressures such as those derived from thermal infrared measurements and cloud lidars. Based on preliminary comparisons with MODIS, we find the effective cloud pressures (CloudPressure) to be on average about 250 hPa higher than the physical cloud-top. These numbers are consistent with previous studies using different instruments (for example, GOME/ATSR).

The original (pre-launch) estimates of the accuracy and precision of the effective cloud pressure retrieval were 100 and 30 hPa, respectively. Preliminary comparisons with MODIS (Joiner, et al., 2004; Vasilkov et al., 2004; Joiner and Vasilkov, 2006; Vasilkov et al., 2008) and the Cloud Physics Lidar (CPL) (Joiner et al., 2006) and more recently with CloudSat (Vasilkov et al., 2008) are consistent with radiative transfer calculations that show enhancement in scattering from multiple cloud decks (which may occur frequently) and significant light penetration into physically thick clouds, especially deep convective clouds. Based on these comparisons and considerations, we believe that our original error estimates are reasonable for optically thick clouds ($\tau > 20$) and for lower τ at Solar Zenith Angles (SZA) near 45 degrees. However, at lower τ and higher and lower SZA, the retrieved cloud pressures may have significant errors, but they should still be sufficiently accurate for use in trace gas retrievals.



4.6.2 Algorithm Quality Assessment

1. In Version 1.0 of OMCLDRR, we used the spectral range 392-398 nm. We found that this fitting window had some undesirable features including (1) sensitivity to Raman scattering in the ocean, (2) significant sensitivity to non-Lambertian behavior of clouds and ground including cloud shadowing, thin cloud phase function, and non-Lambertian behavior of the surface (for example, sea glint), and (3) problems with the MLER model in the presence of thin/broken clouds that produced too low and sometimes negative cloud pressures. In Version 1.1 and beyond, we use the fitting window 346-354 nm. There is significantly more Rayleigh scattering at these wavelengths that mitigates—but does not completely eliminate—problems associated with all of the features mentioned above. Due to the change in the fitting window, OMCLDRR now uses the UV-2 channel to derive cloud pressure, cloud fraction, and reflectivity. This has an added benefit that the cloud fields will have slightly better co-registration with other OMI products (ozone, BrO, and HCHO) that use the UV-2 channel.
2. Under low cloud fraction conditions ($< \sim 0.3$), sea glint can cause erroneously high values of retrieved reflectivity and low values of cloud pressure. Sea glint primarily affects the west side of a swath at low and mid-latitudes. The sea glint possibility flag is contained in bit 4 of the ground pixel quality flag. As mentioned above, cloud pressures are much improved in v1.1 over sea glint conditions.
3. Over snow/ice, the processing quality flag bit 5 is set to 1, and the cloud fraction is assigned to 1. Therefore, the effective cloud pressure for these pixels is representative of an average scene pressure (that is, the LER pressure of a pixel that produces the observed amount of Raman scattering). This is done for a more positive identification of the existence of thick clouds over snow/ice. This is of interest for the retrieval of ozone and other trace gases as well as the calculation of surface UVB. The snow/ice information comes from the Near real-time Ice and Snow Extent (NISE) product created using passive microwave data. It is provided by the National Snow and Ice Data Center (NSIDC) and is included in the Level 1b data set.
4. As the cloud fraction tends to zero, the error in retrieved cloud pressure increases rapidly. These errors can occur in some cases where cloud fractions are very low (approaching 20%). Therefore, for cloud fractions $< 5\%$, we do not attempt a cloud pressure retrieval. Instead, an effective scene pressure is reported for diagnostic purposes only. These cases are indicated where bit 13 of the processing quality flag is set to 1. Retrievals for cloud fractions $< 20\%$ are considered to be suspect and should be used with caution.
5. Transient events due to radiation hits on a detector may produce striping in the cloud pressures (for example, anomalously low or high values at one scan position). This may last only for a short period or may continue until elevated dark currents are adjusted in the calibration; these adjustments are made daily in Collection 3. Transient data are currently flagged in the Level 1b data set. OMCLDRR has the option of checking this flag. However, the default is currently



- not to check the flag. When the transient flag is checked, the algorithm disregards affected transient pixels as well as pixels affected by other types of errors within the fitting window. In practice, we found that the transient flags are set very infrequently and our internal quality control checks are able to detect affected pixels most of the time. When any type of warning or error occurs for pixels within the fitting window for radiance or irradiances, bits 9-12 of the processing quality flag are set as appropriate.
6. Absorbing aerosol in and above clouds can affect the OMCLDRR data. In general, it will reduce the cloud fraction and pressures. The presence of absorbing aerosols is currently not flagged in the OMCLDRR file. The aerosol index flag in the OMTO3 file can be used to check for the existence of absorbing aerosol within a pixel.
 7. Version 1.4 uses a surface albedo climatology based on TOMS. Previous versions assumed a surface reflectivity of 15% consistent with OMTO3. With this change and additional changes in the instrument calibration in Collection 3, we find the cloud pressures to be higher on average than in previous versions, particularly at low cloud fractions.

4.6.3 Additional Information

Questions related to the OMCLDRR dataset should be directed to the GES DAAC. Users interested in these parameters, or having other questions regarding the OMCLDRR dataset, are advised to contact Alexander Vasilkov (alexander_vassilkov@ssaihq.com) and Joanna Joiner (Joanna.Joiner@nasa.gov), who has the overall responsibility for this product.

For more information on this product, refer to:
http://hyperion.gsfc.nasa.gov/People/Joiner/OMCLDRR_README.htm.



4.7 OMI/Aura DOAS Total Column Ozone (OMDOAO3)

4.7.1 Quality Assessment

Validation was performed by comparing the OMDOAO3 total ozone data Version 1.0.1 with collocated Brewer data for the Northern hemisphere, for November 2004 (Veeffkind et al., 2006) as well as for the period between March 28 and June 11, 2005. On average, the retrieved ozone column is biased by 2 % with respect to the Brewers, the standard deviation on this number is 3.5%. The validation results show that the errors increase with increasing Solar zenith angle. In the current version of OMDOAO3 (1.0.5) the Solar zenith angle dependent bias is expected to be much smaller. This is confirmed by comparing to the OMTO3 Collection 2 dataset.

Several papers on the validation of the OMDAO3 data product v1.0.1 will be part of a special issue of the *Journal of Geophysical Research* on the validation of Aura data products, to appear early 2008. We will continue to work on the validation of the Collection 3 Version 1.0.5 data.

To assess the quality of the individual retrievals it is very important to look at the quality flags fields in the data products. The ProcessingQualityFlags are especially important to filter out bad quality data. The best quality data have a ProcessingQualityFlags of 0. It is recommended to apply a bitwise AND on the ProcessingQualityFlags field using a value of 10911 to filter the data. This will filter all data, for which the ProcessingQualityFlags bit 0, 1, 2, 3, 4, 7, 9, 11 and/or 13 are set.

4.7.2 Additional Information

Questions related to the OMDOAO3 dataset should be directed to the [GES DISC](#). For questions and comments related to the OMDOAO3 algorithm and data quality, please contact omdoao3@ltpmail.gsfc.nasa.gov.

For more information on this product refer to:
http://disc.sci.gsfc.nasa.gov/Aura/OMI/omdoao3_v003.shtml



4.8 OMI/Aura Formaldehyde (HCHO) Total Column (OMHCHO)

4.8.1 Quality Assessment

Fitting uncertainties for the HCHO slant columns typically fall within the 40-100 % range, with the lower end of this range over HCHO hot-spots. This is roughly comparable to what has been achieved from GOME. Uncertainties in the air mass factor (AMF), which is used to convert slant to vertical columns, are estimated to be 30 %. Hence, the total uncertainties of the HCHO vertical columns typically fall within the 50-105 % range.

Other quality issues remain the same as for BrO (OMBRO).

4.8.2 Additional Information

For questions and comments related to the OMHCHO algorithm and data quality, please contact Thomas P. Kurosu (tkurosu@cfa.harvard.edu). Please send a copy of your e-mail to Kelly Chance (kchance@cfa.harvard.edu), who has the overall responsibility for this product.

For more information on this product, refer to:

http://www.cfa.harvard.edu/~tkurosu/SatelliteInstruments/OMI/PGEReleases/READMEs/OMHCHO_README.pdf



4.9 OMI/Aura Nitrogen Dioxide (NO₂) Total and Tropospheric Column (OMNO₂)

4.9.1 Quality Assessment

The quality of the OMNO₂ data in this public release is currently being established by independent measurements in ongoing validation campaigns from ground-, aircraft-, and satellite-based instruments. Data quality issues are described in the Data Quality document found at http://toms.gsfc.nasa.gov/omi/no2/OMNO2_data_quality.pdf.

An overview of some of the validation efforts may be found in the presentation http://earth.esa.int/workshops/atmos2006/participants/330/pres_330_kroon.pdf.

Stratospheric amounts are in reasonable agreement with climatological measurements from the Halogen Occultation Experiment (HALOE) instrument aboard the Upper Atmosphere Research Satellite (UARS) and with model calculations from the NASA/GSFC chemical transport model (CTM). Tropospheric amounts are generally consistent with the GEOS-CHEM model (refer to “Section 1.2 Acronyms, Abbreviations,” beginning on Page 1, for Acronym meaning) and indicate prominent sources near urban areas.

The data product includes estimates of uncertainties associated with the various geophysical quantities. The uncertainty estimates have been improved since the provisional release of the OMI data. However, these estimates may not account for all actual sources of random or systematic errors. We anticipate further improvements through the validation process and in understanding the probability distributions of the underlying data and the algorithmic sensitivity to the data.

4.9.2 Additional Information

For questions and comments related to the OMNO₂ algorithm and data quality, please contact omno2@ltpmail.gsfc.nasa.gov. Additional questions may be directed to the principal points of contact for OMNO₂:

James F. Gleason (James.F.Gleason@nasa.gov) and
J. Pepijn Veefkind (veefkind@knmi.nl).

For more information on this product, refer to:

http://toms.gsfc.nasa.gov/omi/no2/OMNO2_readme.pdf
http://toms.gsfc.nasa.gov/omi/no2/OMNO2_release_notes.pdf
http://toms.gsfc.nasa.gov/omi/no2/OMNO2_data_quality.pdf
http://toms.gsfc.nasa.gov/omi/no2/OMNO2_data_product_specification.pdf



4.10 OMI/Aura Chlorine Dioxide Slant Column (OMOCLO)

4.10.1 Quality Assessment

Fitting uncertainties for the OCIO slant columns typically fall within the 40-100 % range, with the lower end of this range within the Antarctic polar vortex where OCIO is most abundant. More details on algorithm specifics can be found in the *OMI Algorithm Theoretical Basis Document*, Volume 4, and in Kurosu et al., 2004.

Other quality issues remain the same as for BrO (OMBRO).

4.10.2 Additional Information

For questions and comments related to the OMOCLO algorithm and data quality, please contact Thomas P. Kurosu (tkurosu@cfa.harvard.edu). Please send a copy of your e-mail to Kelly Chance (kchance@cfa.harvard.edu), who has the overall responsibility for this product.

For more information on this product, refer to:

http://www.cfa.harvard.edu/~tkurosu/SatelliteInstruments/OMI/PGEReleases/READMEs/OMOCLO_README.pdf

4.11 OMI/Aura Sulfur Dioxide Total Column (OMSO2)

4.11.1 Quality Assessment

The accuracy and precision of the SO₂ data vary significantly with the SO₂ loading and vertical profile, observational geometry, slant column ozone, and in the presence of sub-pixel clouds and aerosols. Due to the combination of a smaller footprint and measurements at wavelengths that are highly sensitive to SO₂ absorption, the minimum SO₂ mass detectable by OMI is two orders of magnitude lower than the detection threshold of TOMS (Krueger et al 1995: <http://toms.umbc.edu>).

Details about software versions and known issues are available in the OMSO2 Release Details file (<http://so2.umbc.edu/omi/Documentation/OMSO2ReleaseDetails.html>).

Instrument calibration, forward model, and OMTO3 retrieval errors in the residual wavelengths are compensated by subtracting the median residual in SO₂-free background pixels from the observed residuals. The median is computed for each viewing angle from a sliding group of 350 pixels along the orbit track. SO₂-contaminated and bad pixels are excluded from the median calculation if the OMTO3 error flag is equal to or greater than 5. In addition, BRD pairs that are consistent with real SO₂ and with slant column SO₂ greater than 2 DU are excluded.



Separate Quality Flags (QFs) are provided for each of the products that are based on SO₂ consistency criteria between the individual wavelength pairs. The OMSO2 pixel quality flag is an automatic assessment of the SO₂ values for the corresponding pixel by the OMSO2 retrieval algorithm. It is used primarily as an indicator of the validity of the retrieved SO₂ values. A user of OMSO2 data is advised to examine the first bit of the quality flag. If this bit is equal to zero, the retrieved SO₂ value is likely to be good. However, if it is equal to 1, this indicates that during the retrieval, the algorithm has determined that the pixel does not exhibit characteristics that are consistent with the presence of SO₂. Also the quality flag includes other information, such as the geometrical and geophysical conditions, that are relevant to the quality of SO₂ retrieval. For detailed information about the SO₂ quality flag, please consult the OMSO2.fs file specification (<http://so2.umbc.edu/omi/Documentation/OMSO2.fs.html>).

The pixel quality flags in OMSO2 are not yet fully functional. Preliminary analysis of the QF values has shown that they work best for large volcanic events, but miss many real Planetary Boundary Layer (PBL) and low-level degassing emissions. **Users are advised to ignore QF and use independent verification of PBL SO₂ emissions.**

Below are data quality assessments for each SO₂ product after applying moving median residual correction and ignoring QF. For all data, the noise level in the south Atlantic radiation anomaly is increased.

PBL Data

The slant column (SC) PBL SO₂ data produced with the BRD algorithm feature a practically zero global mean bias (typically within 0.1 DU) and a global background noise level of about 0.6 DU (1 standard deviation) based on a preliminary survey of the data. Using a constant AMF of 0.36, this translates into a ~0.2 DU bias and 1.7 DU noise in global total SO₂ values, while regional noise levels vary significantly. With this sensitivity, daily detection of plumes from strong volcanic degassing and anthropogenic sources of SO₂ (such as smelters and coal burning power plants) are possible. However, any individual SO₂ value for a specific pixel may be questionable due to the large standard deviation of PBL SO₂ values. Therefore, at least weekly or longer time period maps of PBL SO₂ are of greater value, but artifacts are still possible.

We provide diagnostic information in the OMSO2 product, intended to help distinguish real PBL SO₂ signals from artifacts. For example, SO₂ can be computed independently from each of the BRD pairs and the difference between pair solutions would indicate errors in the calibration or retrieval assumptions, or unusual meteorological situations. Comparison between SO₂ data produced with BRD (PBL data) and LF (5km and 15km data) algorithms is also recommended when possible to confirm the presence of SO₂. In unclear cases PGE developers will provide off-line verifications using Spectral Fit (SF) algorithm upon user request (see contact information).



Assuming that detected SO_2 is real, additional errors arise if observational conditions differ from those assumed in the AMF parameterization. For example, an AMF of 0.36 is underestimated by 20 % for $\text{SCO}=700$ DU (small ozone, solar zenith and nadir angles), but overestimated by ~ 30 % for $\text{SCO}=1500$ DU. For even larger SCO values (high ozone and/or high solar and viewing angles, mostly at high latitudes), the AMF becomes very small, so no good PBL SO_2 retrieval is expected. Therefore, fill values are reported for pixels with $\text{SCO}>1500\text{DU}$.

In addition, aerosols and sub-pixel clouds can affect the AMF in different ways depending on their location. The assumption is that clouds always screen PBL SO_2 , but no AMF correction is attempted to account for this invisible SO_2 . This cloud-related AMF error becomes larger with increasing sub-pixel cloudiness, so that fill values are used if the OMTO3 cloud fraction is larger than ~ 20 %, which corresponds to LER ~ 30 %. **Even for low reflectivities, off-line AMF corrections should always be considered before using OMI SO_2 data for estimating SO_2 emissions.**

Useful examples of the recommended AMF corrections are given in OMSO2 AMF corrections file (<http://so2.umbc.edu/omi/Documentation/OMSO2AMFcorrections.html>). We will also provide off-line AMF corrections upon user request.

Volcanic 5 km Data

The 5 km retrievals are intended to represent typical volcanic outgassing from tall volcanoes and emissions from effusive eruptions. We recommend that the 5 km retrievals be used for volcanic degassing cases at all altitudes because the PBL retrievals are restricted to clear sky situations and contain large artifacts when sub-footprint clouds are present. The cloud-related fill values are possible in 5km data when the assumed cloud top (from OMTO3 climatology) is higher than 10 km. In such cases the cloud blocks most of the 5KM SO_2 . As a result, SO_2 weighting function becomes close to zero, no LF retrieval is done, and the fill value is stored in the output. Examples are given in OMSO2 Release Details file <http://so2.umbc.edu/omi/Documentation/OMSO2ReleaseDetails.html>.

In general, SO_2 releases at altitudes less than 5 km will be underestimated due to errors in the AMF, but these could be corrected in an off-line processing if degassing altitude is known. Biases in the 5 km retrievals due to latitude and viewing angle are removed to the 0.1 DU level by the median residual background offset corrections. The standard deviation of 5 km retrievals in background areas is about 0.3 DU at low and mid-latitudes. Both the bias and standard deviations increase for solar zenith angles greater than 80° . Cross-track striping has been found near the northern terminator in some orbits. The known artifacts in the OMTO3 residuals are due to:

- Ozone profile errors in anomalous meteorological situations, for example, cut-off low-pressure systems at mid-latitudes (negative SO_2 errors of ~ -1 DU)
- The possible errors in the cloud top pressure used in the retrieval of total ozone in OMTO3 algorithm.



Volcanic 15 km Data

The 15 km retrievals are intended for use with explosive volcanic eruptions where the cloud is placed in the upper troposphere or stratosphere. At these altitudes the AMF is weakly dependent on altitude, so that differences in actual cloud height from 15 km produce only small errors.

The biases with latitude and viewing angle are generally less than 0.1 DU. The noise level in background data is about 0.2 DU. Both the bias and standard deviation increase near the northern terminator, similar to but reduced from the 5 km results. Artifacts due to ozone profile errors and cloud edges are reduced from the 5 km data by about 30 %. One should see no fill values due to cloud screening in the 15KM data.

The LF algorithm still has large error when it comes to high SO₂ loading cases. The LF algorithm as implemented in the Version 1.0.7 OMSO₂ is expected to provide good retrieval when SO₂ loading is less than ~30 DU. When SO₂ loadings are higher than ~50 DU, the LF algorithm underestimates the true SO₂ amount. The higher the loading is, the larger the underestimation.

4.11.2 Additional Information

Several articles are published about OMSO₂ products (Carn et al, 2007a; Carn et al, 2007b; Krotkov et al., 2007a; Krotkov et al., 2007b; Yang et al., 2007).

For questions and comments related to the OMSO₂ algorithm and data quality, contact Nickolay Krotkov (Nickolay.A.Krotkov@nasa.gov) who has the overall responsibility for this product and send copies to Kai Yang (Kai.Yang.1@nasa.gov), Arlin J. Krueger (akrueger@umbc.edu) and Simon Carn (scarn@umbc.edu).

For more information on this product, refer to:
<http://so2.umbc.edu/omi/Documentation/OMSO2Readme.html>.

4.12 OMI/Aura Ozone (O₃) Total Column (OMTO3)

4.12.1 Quality Assessment

Overall the quality of total ozone and AI data produced by OMTO3 is similar to that from TOMS (<http://toms.gsfc.nasa.gov/>), except for cloudy observations. Based on experience with TOMS, the total ozone data provided in OMTO3 should have a root-mean squared error of 1-2%, depending on solar zenith angle, aerosol amount, and cloud cover. These errors are best described as pseudo-random: systematic over small areas with a unique geophysical regime, random over large areas containing a mixture of geophysical regimes. Preliminary analyses show that OMTO3 data compare about as well with Dobson and Brewer stations as did Nimbus-7/TOMS data. (The overall quality of EP/TOMS data is poorer compared to both Nimbus-7 TOMS and OMI. The EP/TOMS total ozone data have been reprocessed recently by applying an empirical correction,



developed using NOAA/SBUV-2 data, to remove several poorly understood instrument anomalies. The AI data from EP/TOMS, however, have not yet been corrected.)

4.12.2 Additional Information

For questions and comments related to the OMTO3 algorithm and data quality, please contact Kai Yang (Kai.Yang-1@nasa.gov). Please send a copy of your e-mail to P.K. Bhartia (pawan.bhartia@nasa.gov), who has the overall responsibility for this product.

For more information on this product, refer to:

<http://toms.gsfc.nasa.gov/omi/OMTO3Readme.html>

<http://disc.gsfc.nasa.gov/Aura/OMI/omto3.html>

4.13 OMI/Aura Surface UV Irradiances (OMUVB)

4.13.1 Quality Assessment

The radiative transfer model assumes that clouds are plane parallel and homogeneous, that is, it does not account for broken, multi-layer or mixed phase clouds. This error is the principal source of noise in comparing satellite measurements with ground-based instruments. The OMI surface UV irradiance represents the spatial average over the OMI footprint. For each swath, OMI measurements are made once a day around 1:45 p.m. local time. No correction is made for the change in cloudiness, ozone and aerosols between local noon and satellite overpass time, or for their diurnal variability. Previous validation studies with TOMS data suggest that OMI UV irradiance estimates are, on the average, 0-30% larger than the ground-based reference data. The OMI surface UV data were compared with spectral ground-based measurement data of Jokioinen (60.8N, 23.5E), Sodankyla (67.4N, 26.6E), Toronto (43.8N, 79.5W), San Diego (32.8N, 117.2W), Ushuaia (54.8S, 68.3W), and Barrow (71.3N, 156.7W). [The validation results, presented in the AGU fall meeting in December 2005](#), imply similar results as the previous validation studies with TOMS surface UV data. The systematic bias can be attributed to absorbing aerosols from natural and anthropogenic sources. Since the soot content of the urban aerosols tend to be highly localized, these errors presumably are also localized and do not necessarily represent the error in the regional estimate of surface UV made by OMI. Snow and ice further complicate the estimation of the surface UV because clouds cannot be distinguished from them. Therefore, in regions with temporary snow or ice or highly heterogeneous surface albedo, the OMI UV irradiance estimates have much higher uncertainty. A future version of the algorithm may use snow cover information to reduce this uncertainty.

4.13.2 Additional Information

Questions and comments related to the OMUVB dataset, the OMI Surface UV algorithm, or data quality should be directed to [Aapo Tanskanen](#).

For more information on this product, refer to

<http://disc.gsfc.nasa.gov/Aura/OMI/omuvb.shtml>.



Chapter 5: OMI Data Access and Use

5.1 Data Format

The majority of the datasets archived at the NASA's Goddard Earth Sciences Data and Information Services Center (GES DISC) are in the Hierarchical Data Format-Earth Observing System (HDF-EOS) format. NASA has adopted this format for standard data product distribution since it is able to handle multiple types of data objects and at the same time is independent of the platform or operating system the file has been created on.

Two versions of the HDF-EOS format, HDF-EOS 2.x (based on native HDF4 format) and HDF-EOS 5.x (based on native HDF5 format), are in use and are usually referred to as HE4 and HE5 format, respectively.

OMI Level 1B data files (radiance, irradiance, and calibration files) are written in HE4 format and OMI Level 2 and Level 3 products (derived geophysical parameters) are in HE5 format. The file names have the extension .he4 and .he5, respectively.

For tools to read HDF-EOS data files, please refer to "Section 5.3 Using OMI Data," Page 48 of this guide and to: <http://disc.gsfc.nasa.gov/Aura/tools.shtml>.

5.2 Accessing OMI Data

Publicly released Version 2 OMI Products are available from GES DISC home page at: <http://disc.sci.gsfc.nasa.gov/Aura/OMI/index.shtml>

Information about new data releases is broadcast at Aura Validation Data Center (AVDC) at: <http://avdc.gsfc.nasa.gov/Overview/news.html>

Information about OMI data products is also available from KNMI web site at: <http://www.knmi.nl/omi/research/product/>



5.3 Using OMI Data

Software and many tools have been developed by the NASA data centers and software developers to read HDF-EOS files. These tools examine and modify the HE4 and HE5 file contents, dump the files, extract the required data objects (images, orbital swath data, gridded data, and tables), display the content, convert files from old HDF format to new format and vice versa, and convert the file into familiar ASCII or binary format. Some of them are described below:

- **HDFview:** The HDFView is a visual tool for browsing and editing HDF4 and HDF5 files. Using HDFView, users can (1) view a file hierarchy in a tree structure; (2) create new file, add or delete groups and datasets; (3) view and modify the content of a dataset; 4) add, delete and modify attributes; (4) replace I/O and GUI components such as table view, image view and metadata view.
- **read_h5:** The software [read_h5](#) is written in the C language. Users will need the HDF5 libraries when compiling the source code. The program allows users to select a parameter, latitude range, and dump the data to screen as an ASCII file.
- **atmos_h5:** The software [atmos_h5](#) is an IDL-based code. This program not only creates the parameter subsets (with the option of converting data to geophysical parameters) and writes in ASCII or binary format, it also displays the quick-look image on the screen and creates a .jpg file.
- **Giovanni:** A web-based on-line visualization and analysis tool developed for display, data mining and direct download of the selected parameter (for Level 2 or Level 3 products).

For a complete list of tools, please refer to: <http://disc.gsfc.nasa.gov/Aura/tools.shtml>.

A good overview on tools to read OMI data, including IDL program code and an IDL level 2 analysis toolkit (CAMA) is available from http://www.knmi.nl/omi/research/product/read_tool_omi_level2.html.

5.4 Example of Usage

1. Go to <http://disc.gsfc.nasa.gov/Aura/tools.shtml>.
2. Click on “OMI-Giovanni.” Two types of OMI online visualization and analysis are available: Aura OMI TOMS-like daily global 1.0° x 1.25° products and Aura OMI Level 2G daily global products (Beta).
3. Click on “JAVA Version” or “Non JAVA Version” of the product of interest.
4. Choose any of the three optional parameters: Column Amount Ozone, UV Aerosol Index, or Effective Surface Reflectivity.
5. Optionally, choose projection type, plot time and time range.
6. Click on “Generate Plot” or “ASCII Output.”

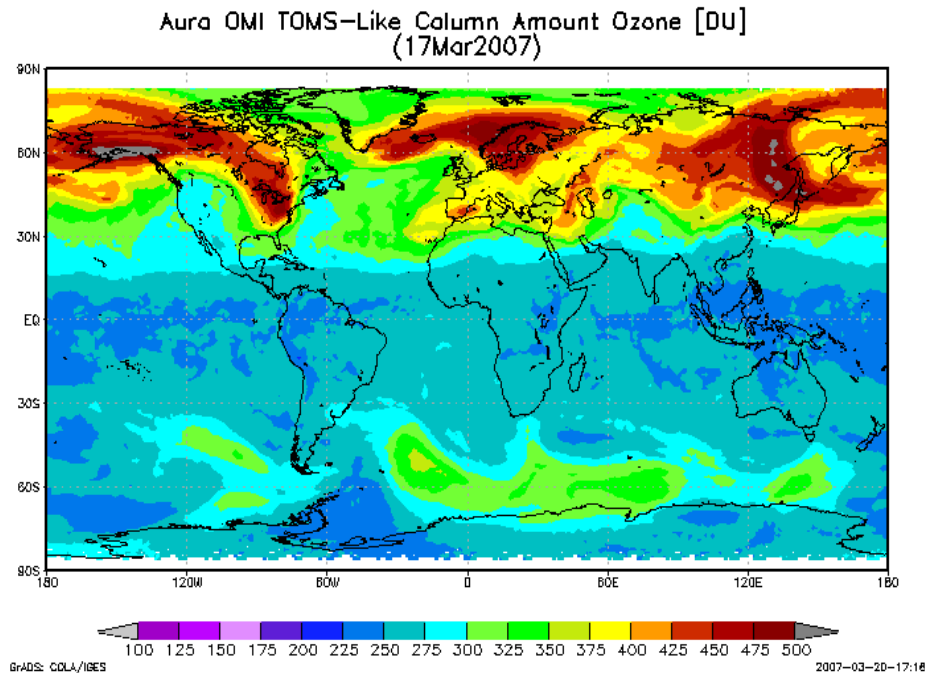


Figure 11: An Image of Column Ozone Generated Using OMI-Giovanni



This page is blank to preserve correct left-right pagination.



Chapter 6: References

6.1 OMI Algorithmic Theoretical Baseline Documents (ATBDs)

OMI ATBD, Volume 1: *OMI Instrument Description and Level 1B Product*

http://eosps0.gsfc.nasa.gov/eos_homepage/for_scientists/atbd/docs/OMI/ATBD-OMI-01.pdf

OMI ATBD, Volume 2: *OMI Ozone Products*

http://eosps0.gsfc.nasa.gov/eos_homepage/for_scientists/atbd/docs/OMI/ATBD-OMI-02.pdf

OMI ATBD, Volume 3: *Clouds, Aerosols, and Surface UV Irradiance*

http://eosps0.gsfc.nasa.gov/eos_homepage/for_scientists/atbd/docs/OMI/ATBD-OMI-03.pdf

OMI ATBD, Volume 4: *OMI Trace Gas Algorithms*

http://eosps0.gsfc.nasa.gov/eos_homepage/for_scientists/atbd/docs/OMI/ATBD-OMI-04.pdf

OMI ATBD, Terms and Symbols

http://eosps0.gsfc.nasa.gov/eos_homepage/for_scientists/atbd/docs/OMI/ATBD-OMI-Terms-Symbols.pdf

6.2 Additional References

KNMI website: <http://www.knmi.nl/omi/research/documents>

Acarreta, J.R. and J.F. de Haan, "Cloud Pressure Algorithm Based on O₂-O₂ Absorption," Algorithm Theoretical Baseline Document: *Clouds, Aerosols, & Surface UV Irradiance*, P. Stammes (ed.), Vol. III, ATBD-OMI-03, Version 2.0, Aug. 2002.

(http://eosps0.gsfc.nasa.gov/eos_homepage/for_scientists/atbd/docs/OMI/ATBD-OMI-03.pdf)

Ahn, C., O. Torres, and P.K. Bhartia, "Comparison of OMI UV Aerosol Products with Aqua-MODIS and MISR Observations in 2006," *J. Geophys. Res.*, submitted manuscript, 2008.



Bhartia, P.K. and C.W. Wellemeyer, "OMI TOMS-V8 Total O₃ Algorithm," Algorithm Theoretical Baseline Document: *OMI Ozone Products*, P.K. Bhartia (ed.), Vol. II, ATBD-OMI-02, Version 2.0, Aug. 2002.

(http://eospsso.gsfc.nasa.gov/eos_homepage/for_scientists/atbd/docs/OMI/ATBD-OMI-02.pdf)

Boersma, F., E. Bucsela, E. Brinksma, and J.F. Gleason, "NO₂," Algorithm Theoretical Baseline Document: *OMI Trace Gas Algorithms*, K. Chance (ed.), Vol. IV, ATBD-OMI-04, Version 2.0, Aug. 2002.

Carn, S.A., N.A. Krotkov, K. Yang, R.M. Hoff, A.J. Prata, A.J. Krueger, S.C. Loughlin, and P.F. Levelt. "Extended observations of volcanic SO₂ and sulfate aerosol in the stratosphere," *Atmos. Chem. Phys. Discuss.*, 7, 2857-2871, 2007.

(<http://www.atmos-chem-phys-discuss.net/7/2857/2007/acpd-7-2857-2007.pdf>)

Carn, S. A., A.J. Krueger, N. A. Krotkov, K. Yang, and P.F. Levelt, "Sulfur dioxide emissions from Peruvian copper smelters detected by the Ozone Monitoring Instrument," *Geophys. Res. Lett.*, 34, L09801, doi:10.1029/2006GL029020, 2007.

Chance, K., T.P. Kurosu, and L.S. Rothman, "HCHO," "OCIO," "BrO," Algorithm Theoretical Baseline Document: *OMI Trace Gas Algorithms*, K. Chance (ed.), Vol. IV, ATBD-OMI-04, Version 2.0, Aug. 2002.

(http://eospsso.gsfc.nasa.gov/eos_homepage/for_scientists/atbd/docs/OMI/ATBD-OMI-04.pdf)

Curier, R.L., J.P. Veefkind, R. Braak, O.Torres, G. de Leeuw, "Retrieval of Aerosols Optical Properties from OMI Radiances Using a Multi-Wavelength Algorithm: Application and Validation to Western Europe," *Journal of Geophysics Research*, 2007.

Dobber, M.R., R. Dirksen, P. Levelt, G.H.J. van den Oord, R. Voors, Q. Kleipool, G. Jaross, M. Kowalewski, E. Hilsenrath, G. Leppelmeier, J. de Vries, W. Dierssen, and N. Rozemeijer, "Ozone Monitoring Instrument Calibration," *IEEE Trans. Geo. Rem. Sens.*, 2006, Vol. 44, No. 5, 1209-1238.

(<http://ieeexplore.ieee.org/search/wrapper.jsp?arnumber=1624601>)

Dutch Space, "Output Products and Metadata," *GDPS Input/Output Data Specification (IODS)*, Vol. 2, SD-OMIE-7200-DS-467, April 9, 2003.

Froidevaux L. and A. Douglass, "Earth Observing System (EOS) Aura Science Data Validation Plan," July 2001.

(http://aura.gsfc.nasa.gov/images/project/aura_validation_v1.0.pdf)

Joiner, J. and A.P. Vasilkov, "First Results from the OMI Rotational Raman Scattering Cloud Pressure Algorithm", *IEEE Trans. Geo. Rem. Sens.*, Vol. 44, No. 5, 1272-1282, 2006. (<http://ieeexplore.ieee.org/search/wrapper.jsp?arnumber=1624606>)



Joiner, J., A.P. Vasilkov, D. Flittner, E. Buscela, and J. Gleason, "Retrieval of Cloud Pressure from Rotational Raman Scattering," Algorithm Theoretical Baseline Document: *Clouds, Aerosols, and Surface UV Irradiance*, P. Stammes (ed.), Vol. III, ATBD-OMI-03, Ver. 2.0, Aug. 2002.

Joiner, J., A.P. Vasilkov, D.E. Flittner, J.F. Gleason, P.K. Bhartia, "Retrieval of Cloud Pressure and Oceanic Chlorophyll Content Using Raman Scattering in GOME Ultraviolet Spectra," *J. Geophys. Res.*, 2004, Vol. 109, D01109.

(<http://www.agu.org/pubs/crossref/2004/2003JD003698.shtml>)

Joiner, J., A.P. Vasilkov, K. Yang, G. Labow, P.K. Bhartia, R. Spurr, M. McGill, G. Heymsfield, L. Li, L. Tian, E. Browell, "Evaluation of OMI Cloud Pressure from Rotational Raman Scattering Using Aircraft and Satellite Data," presented at the Aura Science Team Meeting, Boulder, Colorado, USA, September 11-15, 2006.

(http://code916.gsfc.nasa.gov/People/Joiner/Aura_Val_06_v2.ppt)

Krotkov, N.A., S.A. Carn, A.J. Krueger, P.K. Bhartia, and K. Yang, "Band Residual Difference Algorithm for Retrieval of SO₂ from the AURA Ozone Monitoring Instrument (OMI)," *IEEE Trans. Geo. Rem. Sens.*, Vol. 44, No. 5, 1259-1266, 2006.

([doi:10.1109/TGRS.2005.861932](https://doi.org/10.1109/TGRS.2005.861932))

or (<http://ieeexplore.ieee.org/search/wrapper.jsp?arnumber=1624604>)

Krotkov, N.A., J. Herman, P.K. Bhartia, C. Seftor, A. Arola, J. Kaurola, P. Taalas, and A. Vasilkov, "OMI Surface UV Irradiance Algorithm," Algorithm Theoretical Baseline Document: *Clouds, Aerosols, and Surface UV Irradiance*, P. Stammes (ed.), Vol. III, ATBD-OMI-03, Version 2.0, Aug. 2002.

Krotkov, N.A., A. Krueger, K. Yang, S. Carn, P.K. Bhartia, and P. Levelt, "SO₂ Data from the Ozone Monitoring Instrument (OMI)," in *Proceedings of the ENVISAT Symposium*, 2007, 23-27 April 2007, Montreux, Switzerland (July 2007), H. Lacoste & L. Ouwehand (Eds.), ESA SP-636 //CD (2 volumes).

Krotkov, N.A., B. McClure, R. Dickerson, S. Carn, Can Li, P.K. Bhartia, K. Yang, A. Krueger, Z. Li, J. Hains, P. Levelt, H. Chen, J. Yuan, F. Gong, and X. Bian, "Ozone Monitoring Instrument (OMI) SO₂ validation over NE China," *J. Geophys. Res.*, *AURA Special Issue*, accepted, Nov. 2007, Paper #: 2007JD008818RR.

Krueger, A.J., N.A. Krotkov, S. Datta, D. Flittner, and O. Dubovik, "SO₂," Algorithm Theoretical Baseline Document: *OMI Trace Gas Algorithms*, K. Chance (ed.), Vol. IV, ATBD-OMI-04, Version 2.0, Aug. 2002.

Kurosu, T.P., K. Chance, and C.E. Sioris, "Preliminary Results for HCHO and BrO from the EOS-Aura Ozone Monitoring Instrument," *Passive Optical Remote Sensing of the Atmosphere and Clouds IV*, S.C. Tsay, T. Yokota, and M.-H. Ahn (Eds.), *Proc. of SPIE*,



2004, Vol. 5652 (SPIE, Bellingham, WA, 2004), 0277-786X/04/\$15.
(http://cfa-www.harvard.edu/~tkurosu/Papers/SPIE_2004.pdf)

Levelt, P.F., E. Hilsenrath, G.W. Leppelmeier, G.H.J. van den Oord, P.K. Bhartia, J. Tamminen, J.F. de Haan and J.P. Veefkind, "Science Objectives of the Ozone Monitoring Instrument," *IEEE Trans. Geo. Rem. Sens.*, Vol. 44, No. 5, 1199-1208, 2006.
(<http://ieeexplore.ieee.org/search/wrapper.jsp?arnumber=1624600>)

Torres, O., R. Decae, J.P. Veefkind, and G. de Leeuw, "OMI Aerosol Retrieval Algorithm," Algorithm Theoretical Baseline Document: *Clouds, Aerosols, and Surface UV Irradiance*, P. Stammes (ed.), Vol. III, ATBD-OMI-03, Version 2.0, Aug. 2002.

Torres, O., A. Tanskanen, B. Veihelmann, C. Ahn, R. Braak, P.K. Bhartia, P. Veefkind, and P. Levelt, "Aerosols and surface UV products from Ozone Monitoring Instrument observations: An overview," *J. Geophys. Res.*, 112, D24S47, 2007.
(doi:10.1029/2007JD008809)

Torres, O., C. Ahn, M. Andrade, and T. Eck, "Evaluation of OMI UV Aerosol Products Using AERONET Observations," *J. Geophys. Res.*, submitted manuscript, 2008

van den Oord, G.H.J., R.H.M. Voors, and J. de Vries, "The Level 0 to Level 1B Processor for OMI Radiance, Irradiance and Calibration Data," Algorithm Theoretical Baseline Document: *OMI Instrument, Level 0-1B Processor, Calibration & Operations*, P.F. Levelt (ed.), Vol. I, ATBD-OMI-01, Version 2, Aug. 2002.

van den Oord, G.H.J., J. P. Veefkind, P. F. Levelt, M. R. Dobber, "Level 0 to 1B Processing and Operational Aspects," *IEEE Trans. Geosc. Rem. Sens.* 44 (5), pp 1380-1397, 2006.

van Oss, R.F., R.H.M. Voors, and R.D.J. Spurr, "Ozone Profile Algorithm," Algorithm Theoretical Baseline Document: *OMI Ozone Products*, P.K. Bhartia (ed.), Vol. II, ATBD-OMI-02, Version 2.0, Aug. 2002.

Vasilkov, A.P., J. Joiner, K. Yang, and P.K. Bhartia, "Improving Total Column Ozone Retrievals by Using Cloud Pressures Derived from Raman Scattering in the UV," *Geophys. Res. Lett.*, 2004, Vol. 31, L20109.
(<http://www.agu.org/pubs/crossref/2004/2004GL020603.shtml>)

Vasilkov, A., J. Joiner, R. J. D. Spurr, P. K. Bhartia, P. Levelt, and G. L. Stephens (2008), "Evaluation of the OMI Cloud Pressures Derived from Rotational Raman Scattering by Comparisons with Other Satellite Data and Radiative Transfer Simulations," *J. Geophys. Res.*, doi:10.1029/2007JD008689, in press.



Veefkind, J.P., and J.F. de Haan, "DOAS Total O₃ Algorithm," Algorithm Theoretical Baseline Document: *OMI Ozone Products*, P.K. Bhartia (ed.), Vol. II, ATBD-OMI-02, Version 2.0, Aug. 2002.

Veefkind, J.P., J.F. de Haan, E.J. Brinksma, M. Kroon and P.F. Levelt, "Total Ozone from the Ozone Monitoring Instrument (OMI) Using the DOAS Technique," *IEEE Trans. Geo. Rem. Sens.*, Vol. 44, No. 5, 1239-1244, 2006.
(<http://ieeexplore.ieee.org/search/wrapper.jsp?arnumber=1624602>)

Yang, K., N. A. Krotkov, A. J. Krueger, S. A. Carn, P. K. Bhartia, and P. F. Levelt, "Retrieval of large volcanic SO₂ columns from the Aura Ozone Monitoring Instrument: Comparison and Limitations," *J. Geophys. Res.*, 112, D24S43, doi:10.1029/2007JD008825, 2007.